GEOMETRIC MODELING OF BIO-INSPIRED TOPOLOGICALLY INTERLOCKING SPACE-FILLING SHAPES

A Thesis

by

SAI GANESH SUBRAMANIAN

Submitted to the Office of Graduate and Professional Studies of
Texas A&M University
in partial fulfillment of the requirements for the degree of

MASTER OF SCIENCE

Chair of Committee,	Vinayak R. Krishnamurthy
Co-Chair of Committee,	Ergun Akleman
Committee Members,	Bruce Tai
Head of Department,	Andreas A. Polycarpou

December 2020

Major Subject: Mechanical Engineering

ABSTRACT

Over the past decades, the benefits of segmentation and fragmentation has started gaining the interest of researchers of engineering design community. Fragmented materials in which the individual segments are held together not using a binder or adhesive, but simply through the geometry of constituting shapes and their arrangement are called *topologically interlocking materials*. Such materials has proven to have distinctive properties like energy absorption, fracture toughness and structural integrity compared to monolithic solids. The geometric design space of the existing topologically interlocking shapes has remained limited and we observe that there is no systematic design methodology to design and explore topologically interlocking shapes. We note that this problem is better understood using the conceptual framework of *space-filling* shapes because it helps us create both water-tight (or void-free shapes) and repeatable shapes (that are easy to mass produce). So the aim of our research was to *develop a systematic methodology to design and explore potentially new topologically interlocking shapes that are repeating and fill-space in a water-tight way.*

We inspire our approach from a novel topological shape called 'Scutoid' that are found in skin cells. The presence of this shape minimizes the tissue energy and stabilizes the 3D packing. Scutoids are important to us because they are both watertight and showed some potential for topological interlocking. Scutoids are constructed by a layer-by-layer Voronoi decomposition. We use this fact to generalize and develop an elegant design methodology to design a new class of shapes that did not exist before called 'Delaunay Lofts'. Specifically, the 'Topology shift' or bifurcation that makes Scutoids interesting, happens when a Voroni edge collapses to a four valency Voronoi vertex and splits back to a Voronoi edge. We show that if we use a quad grid as a reference and define control line segments passing through the quad grid, we automatically obtain the bifurcation. Subsequently, we describe how we can use Wallpaper symmetry groups to create repeatable shapes. However, the algorithmic limitations of Delaunay Lofts restricts free-form exploration of control curves and the shapes fails to show significant topological interlocking capabilities.

To overcome this, we developed an algorithm for Voronoi decomposition with higher dimensional Voronoi sites. Further, we take inspiration from Abeille's Vault design from 1699 and propose the design of interlocking shapes by finding a visual correspondence with weave symmetry. Then we do a structural analysis and compare the results of three such topologically interlocking assemblies we get using predefined Voronoi sites. The results show that the tiles have a well-defined stress patterns and stress magnitudes are comparable to that of the equivalent monolothic solid. This research also shows a great potential in the areas of 3D printing in-fills, metamaterial designs, packaging and education applications.

DEDICATION

To my mother *Bhuvaneshwari*,

The person who means everything to me, who loves me no matter what.

To my father *Subramanian*,

For trusting me with all the uncertainties and grounding me to reality.

To my sister *Sai Janani*,

For supporting during times when all I wanted to do was to give up.

To my grandmother *Kamala* and my aunt *Ambu*,

For rejuvenating a childlike curiosity in me.

To my roommates and friends,

For being a family away from home.

ACKNOWLEDGMENTS

"*To sense that behind anything that can be experienced there is a something that our minds cannot grasp, whose beauty and sublimely reaches us only indirectly: this is religiousness. In this sense I am religious. To me it suffices to wonder at these secrets and to attempt humbly to grasp with my mind a mere image of the lofty structure of all there is.*" - Albert Einstein

I joined A&M in August of 2018, without any idea what university life had in place for me. Little did I expect that I will be a part of uncovering design principles to create fundamentally new repeating shapes. I'm grateful to the professors, students, staffs and all others who have been a part of my journey of graduate life. I can't thank Dr. Krishnamurthy enough for nurturing me from how I was, to what I am today. I'm incredibly grateful to him for cultivating my interest and teaching me what it means to pursue meaningful knowledge in every stage of my graduate life. I learned that coming up with new ideas and thoughts is not really tough, but what is challenging is to stay organized and focus your exploration.

It is hard to think of a meeting that I left without being surprised by the enthusiasm and excitement shown by Dr. Akleman. His wide-ranging knowledge, wisdom, his never ending curiosity and energy has never failed to amaze me. It is only due to him that I realized how unjustified, needless it is to spend time on materialistic endeavors. Conversations between Dr. Krishnamurthy and Dr. Akleman, both philosophical and technical have stimulated a passion towards mathematics and geometry. I hope that this passion that would stay with me for lifetime beyond the graduate school. Special thanks to Dr. Tai for helping out with the 3D Printing of our shapes and providing valuable suggestions for structural evaluation. I'd like to extend my thanks to Dr. Jianer Chen for teaching me ideas in Computational Geometry and making me realize the importance of writing out rigorous mathematical proofs to develop and validate algorithms. Overall, it has been my great privilege to get the opportunity to work, learn and grow under the professors who I got a chance to work with.

Next, I'd like to thank all the student collaborators who have helped me bring the best of myself.

Ting-Ju, Ronak and Peng were the first people who welcomed me to the lab and I'm grateful to them for sharing their experiences and advising me to focus on the right things and helping me out with my doubts and clarifications howsoever small they were. There are two Matt's who have been my major collaborators and support pillars during over the two years. Memories of working overnight with Matt Eng on rendering, making edits to the video (and ping pong games in-between) and SIGGRAPH experiences will remain with me forever. Matt Ebert — his calmness and chill attitude has really been such a relieving factor for me during peak submission times.

I'm thankful for getting the best set of friends in College Station and around the world who are always willing to listen to and show interest in what's going on in each other life and sharing knowledge, experience and difficulties. With Ashwath, Naveed, Srivignesh and other people from A&M alongside, I have never every felt or regretted that I'm 10,000 miles away from home. Needless to say my NIT Trichy friends — Amber B32, and B72 groups with whom I have conversations, arguments about any random topic in the world — has always given me something to look up to and contemplate. Lastly, the friends from my school: Viswanath, Rama Srinivas, Jagga, Venky, P Su and others. They know every bit of me and are always there to share my happiness and difficulties. You guys are the people who I look up to, for coming back to India.

Finally, I want to thank my family who has been on the receiving end of my phone calls on a daily basis. I don't know how they managed to listen to all my random thoughts and opinions and I want to take this opportunity to appreciate their patience and unceasing support. I hope I have made them proud and I will try my best to continue to do so.

CONTRIBUTORS AND FUNDING SOURCES

Contributors

This work was supported by a thesis committee consisting of Dr. Vinayak R. Krishnamurthy and Dr. Bruce Tai of the Department of Mechanical Engineering and Dr. Ergun Akleman of the Department of Architecture and Visualization.

Undergraduate student researcher Matthew Ebert, graduate student researchers Matthew Eng, Chi-an Fu, Katherine Boyd provided invaluable contributions during construction, rendering and analysing the shapes.

All other work conducted for the thesis was completed by the student independently.

Funding Sources

The graduate student was supported through a Graduate Research Assistantship as a part of start-up fund by the Texas A&M University and Department of Mechanical Engineering.

NOMENCLATURE

OGAPS	Office of Graduate and Professional Studies at Texas A&M University
TAMU	Texas A&M University
GAT	Generalized Abeille Tiles
FEA	Finite Element Analysis
CSG	Constructive Solid Geometry
B-rep	Boundary Representation
CAD	Computer-Aided Design

TABLE OF CONTENTS

Page

LIST OF FIGURES

1. INTRODUCTION

Naturally occurring materials are fundamentally made of basic components such as proteins, minerals and lipids. These basic components repeat and group together through the process of self-assembly as controlled by living cells to become materials with remarkable functional properties. Also in the macroscopic level, division into a series of repeating segments gives a higher degree of flexibility and mechanical functionalities. Over the past decades, the benefits of segmentation and fragmentation has started gaining the interest of researchers of engineering design community [4]. Fragmented materials in which the individual segments are held together not using a binder or adhesive, but simply through the geometry of constituting shapes and their arrangement are called **topologically interlocking materials**. This design concept enables taking advantage of flexibility provided by segmentation while maintaining the overall structural integrity of the material using interlocking.

According to Estrin et al. [5], "*topological interlocking is a design principle by which elements (blocks) of special shape are arranged in such a way that the whole structure can be held together by a global peripheral constraint, while locally the elements are kept in place by kinematic constrains imposed through the shape and mutual arrangement of the elements.*". Topological interlocking materials has proven to have distinctive properties like energy absorption, fracture

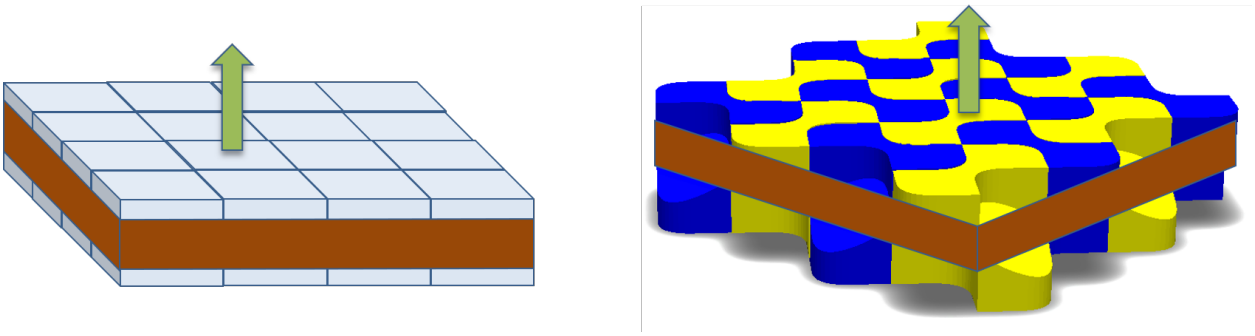

Figure 1.1: Understanding topological interlocking by comparing a cubical assembly (right) with an interlocking assembly generated using our design algorithm (right). The brown tape around the assembly is an elastic band that holds the assembly together.

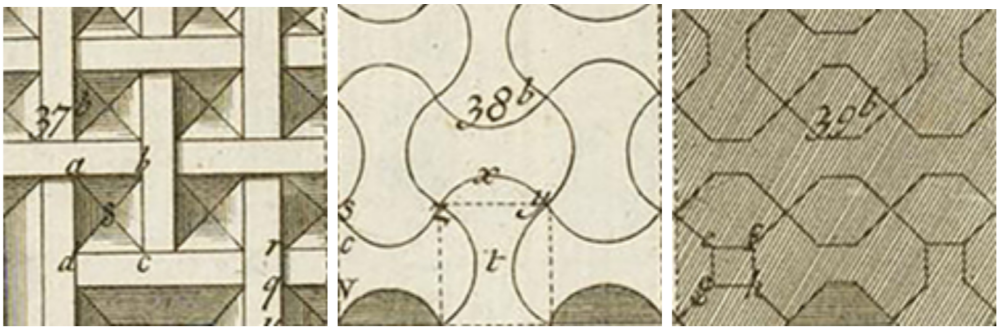

Figure 1.2: Hand-drawn illustrations of 1738 Drawings of top views of Abeille and Truchet vaults by Frezier [1] (left) Top View of flat Abeille vault, (middle) Top View of Abeille vault with circular edges and (right) Top View of a Truchet vault.

toughness and structural integrity compared to monolithic solids [6]. In the research front, the concept of topological interlocking has advanced the design of hybrid materials [4] and materials with adaptive mechanical properties [7]. Shown in Figure 1.1 is an example of topologically interlocking material developed in this research work.

We note that such mechanical properties have only been explored with a limited geometric design space of interlocking shapes. Also, to our knowledge, there is no unified systematic design methodology to create topologically interlocking shapes. Specifically, the geometry of the existing designs are either based on Joseph's Abeille Vault (figure 1.2) or Osteomorphic blocks restricting the design space shapes that can be explored. Particularly, we note that most of the designs have gaps or voids in-between which typically lead to mechanical instabilities as the elements are loosely packed. For this reason, we choose to explore topologically interlocking blocks that are **space-filling**. A space filling shape is a shape that can simply be repeated and packed together to fill the entire $3D$ domain [8, 9] without having any gaps or overlaps in-between them. Space-filling shapes have applications in a wide range of areas from chemistry and biology to engineering and architecture [8]. Using space filling shapes, we can compose and decompose complicated shelled and volumetric structures for design and construction. Furthermore, if a given shape can be uniformly repeated to fill space, it is easier to mass produce using faster methods such as casting and injection molding instead of machining and additive manufacturing several unique shapes.

To date, most widely known space filling shapes are essentially regular prisms (e.g. rectangular bricks) since they are relatively easy to manufacture and are widely available. Reliance on regular prisms, on the other hand, significantly constrains our design space for obtaining reliable and robust structures [10, 11, 12, 13, 14]. Architects currently investigate many other types of space filling modules, but their investigations are not usually systematic and focus on only a small number of known building blocks [15]. We also recognize a need for formal approaches that enable the design and intuitive *control* of a wide variety of modular and tile-able building blocks.

In summary, we aim to *develop a systematic methodology to design and explore (potentially new) topologically interlocking shapes that are repeating and fill-space in a water-tight way.*

1.1 Approach

We inspire our approach from a novel topological shape called 'Scutoid' that are found in skin cells. It was found that the presence of Scutoid minimizes the tissue energy and stabilizes the 3D packing. Scutoids are important to us because they are both watertight and showed some potential for topological interlocking. Scutoids are constructed by a layer-by-layer Voronoi decomposition. We use this fact to generalize and develop an elegant design methodology to design a new class of shapes that did not exist before called 'Delaunay Lofts'. Specifically, we show that the 'Topology shift' or bifurcation that makes Scutoids interesting, happens when a Voroni edge collapses to a four valency Voronoi vertex and splits back to a Voronoi edge. We show that if we use a quad grid as a reference and define control line segments passing through the quad grid, we automatically obtain the bifurcation. Subsequently, we describe how we can use Wallpaper symmetry groups to create repeatable shapes. Then, with the help of FEA of assemblies of Delaunay Lofts, we make two suggestions for designing interlocking shapes. One, the control lines that describe the shape should not be co-planar. Second, grouping of adjacent Delaunay Lofts together may give better topological interlocking.

Inspired from the idea of grouping multiple shapes together, we explore a new class of assemblies called 'Generalized Abeille Tiles' that are ensured to be topologically interlocking. In this effort, we observe a correspondence between structures proposed by Abeille and the symmetries

exhibited by woven fabrics. By configuring these new Voronoi sites based on weave symmetries, we provide a method for constructing topologically interlocking shapes. To construct these shapes, we propose an algorithm for Voronoi decomposition with higher dimensional Voronoi sites. Subsequently, we present a comparative structural analysis of these shapes for three different representative fabric patterns and show the existence of a relationship between the choice of fabric symmetries and the corresponding distribution of stresses in the assembly. Through FEA, we also show the lack of structural stability in the Abeille Vault as opposed to good interlocking capability in the Generalized Abeille Tiles.

Finally, we also a show a rich possibility of future directions that can be inspired by our research in the areas of in-fill design for 3D printing, metamaterial designs, design of reciprocal frames, geometric interlocking, architectural design, heat transfer, air-flow control and education. In the future, our overarching goal is to develop a inverse design system where the user provides force and kinematic conditions and our algorithm generates the geometry automatically. We believe our methodology helps new design space of in-fills and additive manufactured materials in general with adjustable mechanical properties.

1.2 Thesis Overview

The thesis is organized as follows. In Chapter 2 we discuss the existing research work on designing topologically interlocking shapes, its applications in mechanics and architecture and highlight how our research overcomes the limitations. We also provide the necessary mathematical preliminaries in this chapter. In Chapter 3, we introduce Delaunay Lofts, describe the method to create space-filling shapes. Subsequently, we do the structural analysis of assemblies of these Lofts and end by highlighting the limitations of Delaunay Lofts. In Chapter 4, we explain how we can make use of 3D Voronoi partitioning to overcome the limitations of Delaunay Lofts. We then describe how to make use of weave symmetries to create better interlocking shapes that are validated, again, using a structural evaluation. Finally, in Chapter 5, we summarize our contributions, highlight the limitations and discuss the broad future directions of this research pursuit.

2. LITERATURE AND THEORETICAL FOUNDATIONS

2.1 Topological Interlocking

Topological Interlocking assemblies can be held together by boundary or peripheral constraints while locally the elements are kept in place by kinematic constrains imposed through the shape and arrangement of the elements. We find that the idea has been introduced earlier in the context of vault design in architecture more than three centuries ago. But only after it was formally introduced by Dyskin, Estrin and others in the year 2001 [16], this concept started gaining the attention in the mechanics and architecture community. In this section we will provide an overview of the methods used to design these shapes (Section 2.1.1), and highlight the use of these shapes in architecture (Section 2.1.3) and mechanics (Section 2.1.2).

2.1.1 Geometry of Topological Interlocking Blocks

Geometry of topologically interlocking blocks are typically derived starting from the assembly of interlocked tetrahedron-shaped blocks [16]. Assuming a monolayer structure, a research showed that blocks with the outer geometry of any of the five platonic bodies (tetrahedron, cube, octahedron, dodecahedron, and icosahedron) are interlockable [17]. These arrangements can be truncated using a number of planes parallel to the middle plane are the shape are still interlockable [18]. Another range of interlocking blocks can be obtained from these basic ones using transformation [19, 20]. There are also a number of other design that are merely a parametric variation of these designs with curved and other polygonal surfaces. For example, a research showed circle-based and octagon-based interlocking shapes [21]. We note that all these blocks are not space-filling and the tiled assembly of these blocks have voids or unevenness in the assembly.

The first class of space-filling topologically interlocking blocks were discovered in the early 2000s are are called ‘osteomorphic’ blocks (that derives its name because of similarities with a bone). The ability of these blocks to be interlocking within a structure is because of their matching concavo-convex contact surfaces [22]. These blocks are studied extensively in mechanics (see sec-

tion 2.1.2) and are used for range of applications from space shuttle [23] to road construction [24]. we note that the increase study of these blocks is due to fact that they are space-filling and offer a neat way to decompose a solid block into segments unlike the interlocking shpaes based on platonic solids. But geometrically, the design of these blocks are parametric and thus the design space of these blocks are limited.

Thus, we observe that the true potential of Topological Interlocking has not been completely realized in the context of geometric modeling and design of complex structures. This is because there seems to be no systematic way to discover similar building blocks. Moreover, most of these structures are not space-filling. There is, therefore, a need for formal approaches that enable intuitive design and *control* of a wide variety of modular and tileable building blocks. Our motivation is to cater to this need by developing and investigating a methodology to expose the vast design space of topological interlocked space-filling shapes.

2.1.2 Significance in Mechanics

In the Section 2.1.1 we noted that decomposition of a monolithic block into segments will give us void-free packing of the segments. Here, we highlight that such topological interlocking materials have came out to be materials with properties that are not ordinarily found in a monolithic solids [6]. Segmenting a monolithic block into individual blocks has a number of advantages including energy absorption, fracture toughness and structural integrity.

Segmenting a monolithic solid may, in fact, lead to better mechanical properties (especially toughness). This is known as the inverse scale effect. This is confirmed by the Weibull statistics which says that the probablity of survival of a solid is inversely affected with increasing volume [25]. Also, Ashby and Bréchet [4] showed that with increasing brittleness of the material, the effect of segmentation increases. Since, any method that we use to create topologically interlocking shapes can be seen as a segmentation if the shapes are space-filling, our designs will automatically have these mechanical properties.

Another interesting mechanical property of these materials is the controlability of bending stiffness of the material simply by varying the magnitude of peripheral load (that we give in the

elastic band in Figure 1.1. Intuitively, the force required to pull the block out of the assembly will become increasingly tougher if you tighter the elastic band that holds together the boundary of assembly. In fact, an empirical relation for the force necessary to remove a block from the assembly was developed where the required force is proportional to the constraining force from the elastic band [26]. So, the bending stiffness of the assembly can be controlled by changing the constraining load over time. Researchers have developed different ways of implementing the peripheral load including a lateral load using built frames and tension cables [27, 28].

Perhaps the most useful property of Topologically Interlocking Assemblies that are is extensively studies is to resist the growth of cracks. In a topological interlocked assembly, since the blocks are not bonded to each other, boundaries between them are able to hinder crack propagation. While in a monolithic solid crack propagates all the way to the boundary simply because it is a continuous region. This inherently increases the fracture toughness of topologically interlocking solids. The mechanism of controlled crack propagation in segmented solids was experimentally verified and studies in a number of research works [22, 29, 30, 31, 32, 33].

2.1.3 Significance in Architecture

The primary inspiration to explore Topological Interlocking came from Joseph Abeille's 'Abeille vaults' that was discovered during the late 17th Century [34] (See Figures 4.2b). Abeille vaults are stones, generated by truncating two opposite edges of a tetrahedron, that can be assembled in a two-directional pattern to form self-supporting structures [35, 36]. Since then, several variants of these structures have been invented and studied under the name of topological interlocking assemblies (TIA) [16, 37, 38, 5]. These assemblies typically consist of a single unit element that can be repeatedly arranged in such a way that the assembled structure composed of this element can be held together by boundary constraints. Furthermore, each element itself is kept in place by local kinematic constrains imposed through the shape and mutual arrangement of the elements [16].

Medieval building masters have employed assemblies similar to Abeille's vaults. Early examples of similar assemblies, which are usually referred as stereotomy, can be found in Villard de Honnecout's fylfot grillage assemblies, Leonardo da Vinci's spatial structures, Sebastiano Serlio's

planar floors, and John Wallis's scholarly work [39]. In these constructions a discrete load-bearing element supports two neighboring components, and is mutually supported by two others to span distances longer than their length [40, 41]. Abeille's vault was patented at the end of the 17th century as a class planar assemblies that could overcome the structural instability under the application of loads that are perpendicular to planar surface [42]. Other related terms topological interlocking are stereotomy [43, 35] and reciprocal frames or nexorades [44], which are used to refer ancient Asian forms of timber construction [45].

Sébastien Truchet discovered and patented another topologically interlocked module as a variant of Abeille's vault again using identical blocks in early 18th century [46, 15]. One of the advantages of both Abeille's and Truchet's patents is their ability to sustain loads and control the displacement of the blocks [47]. Both of these structural systems are capable of tolerating orthogonal and transverse forces [48]. However, for these assemblies to work the whole assembly process must be completed. Moreover, these assemblies require strong boundary support provided by structures such as buttresses or hefty walls [47]. Therefore, Abeille's shapes and their derived versions never really gained much popularity [49, 41] and were primarily used to build only a few flat vaults in Spain during late 18th and early 19th century [50]. It is only in recent literature that Abeille's creations received a renewed attention mainly in material design and architecture communities [51, 15]. Even then, most current research has only focused on either analyzing existing building blocks already proposed by Abeille and Truchet or creating curved structures from originally known blocks [46, 15]. As a result, even the physical evaluation of such structures remains limited to the original Abeille blocks.

2.2 Space Filling Shapes

A space filling shape is a cellular structure whose replicas together can fill all of space watertight, i.e. without having any voids between them [8]. Equivalently, a space filling shape is a cellular structure that can be used to generate a tessellation of space [9]. While 2D tessellations and space filling shapes are relatively well-understood, problems related to 3D tessellations and space filling shapes are interesting and have applications in a wide range of areas from chemistry

and biology to engineering and architecture [8].

A well-known anecdote to demonstrate the difficulty of 3D tessellations is that Aristotle claimed that the tetrahedron can fill space. Several efforts were made to prove his claim [52] only to find that cube is the only space filling Platonic solid [53]. Goldberg exhaustively catalogued many of known space-filling polyhedra with a series of papers from 1972 to 1982 such as [54, 55, 56]. There are only eight space-filling convex polyhedra and only five of them have regular faces, namely the triangular prism, hexagonal prism, cube, truncated octahedron [57, 58], and Johnson solid gyrobifastigium [59, 60]. It is also interesting that five of these eight space filling shapes are "primary" parallelohedra [61], namely cube, hexagonal prism, rhombic dodecahedron, elongated dodecahedron, and truncated octahedron.

There have been many works in interpolations of tilings in 2D space[62, 63, 64, 65]. Recently, there has been interest in the mechanical characterization of 3D printed 2D tilings in the context of “sheet materials” as well [66]. In this case, the sheet material is only a thin extrusion of a two-dimensional tiling. Two interesting cases of 2D tilings relevant to our approach are those presented by Kaplan [67] showing a wide variety of artistic patterns using specific Voronoi site configurations and Rao [68] that show a systematic construction of 2D pentagonal tilings. In fact our work, in a sense, expands on these two works to move beyond tilings in 2D space to a rich design space of tilings in 3D space.

2.3 Theoretical Foundations

In this section, we provide the basic foundations for our approach. All the information in this section is well known. We only provide it to establish a context for our approach. This background will also provide a foundation for the development of algorithms to construct space-filling tiles in 3D space.

2.3.1 Voronoi Diagrams

Voronoi diagrams are well known geometric structures that are used for diverse applications. Given a set of sites in a domain, voronoi diagram partitions the plane into separate regions based

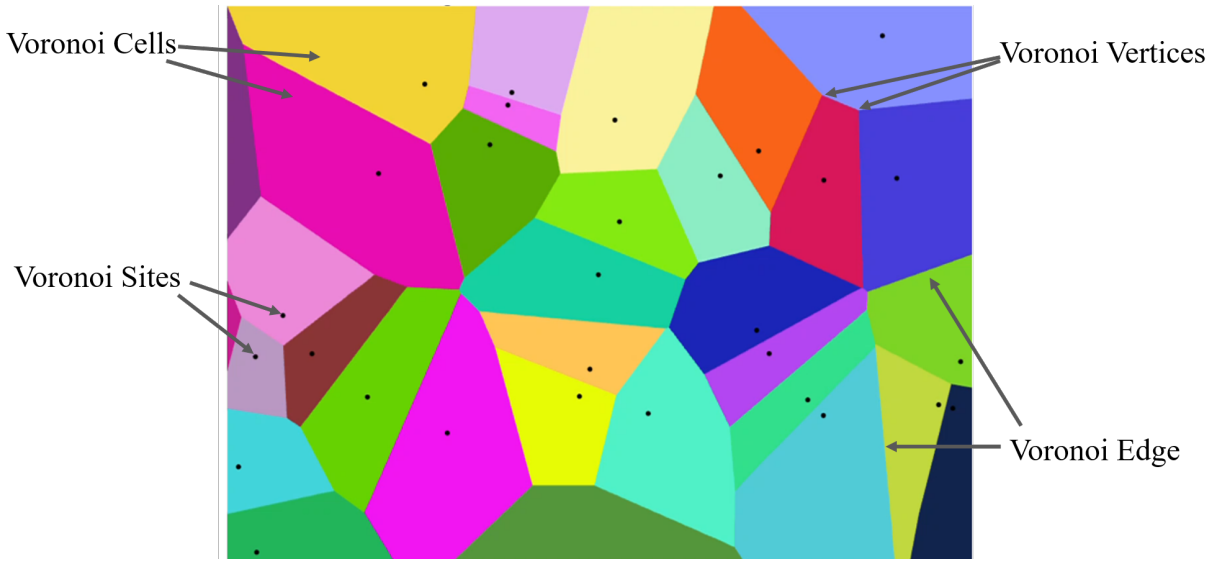

Figure 2.1: Voronoi diagram is a partitioning of a plane into regions based on points (marked as voronoi sites) in a way such that each points take the area closest to it when compared with the neighboring sites. The boundary edges that are formed are called voronoi edges and the points where the edges intersect are called voronoi vertices. An important characteristics of Voronoi vertices is the valency associated with it. Valency of a vertex is the number of edges intersecting at the vertex. In this example, we have a random distribution of Voronoi points and all the vertices have a valency of 3.

on the distance to these sites. The voronoi diagram of n Voronoi sites, is a partition of the domain into n regions where each site in the domain is associated to a region that contains all the points in the plane that are closer to site itself than to any other site. This simple idea of site-based segmentation of a given domain finds its use in wide ranging application ranging from biology (for modelling cells and bone micro-architecture [69]) hydrology (calculating rainfall of an area) in Natural Sciences, to polymer physics (representing free volumes of polymers), aviation (oceanic plotting charts) and architecture in Engineering to name a few.

Considering complete generality, we can extend our thinking to a set of objects in a n-dimensional space and find its Voronoi partitioning of n-d space based some generalized metric. For practical applications such as CAD, shape recognition, topological skeleton, medial axis, volume segmentation [70] or any other computer graphics application, we mostly deal with 3D objects. Although the idea behind creating Voronoi diagrams is simple, it decomposes the domain into shape that

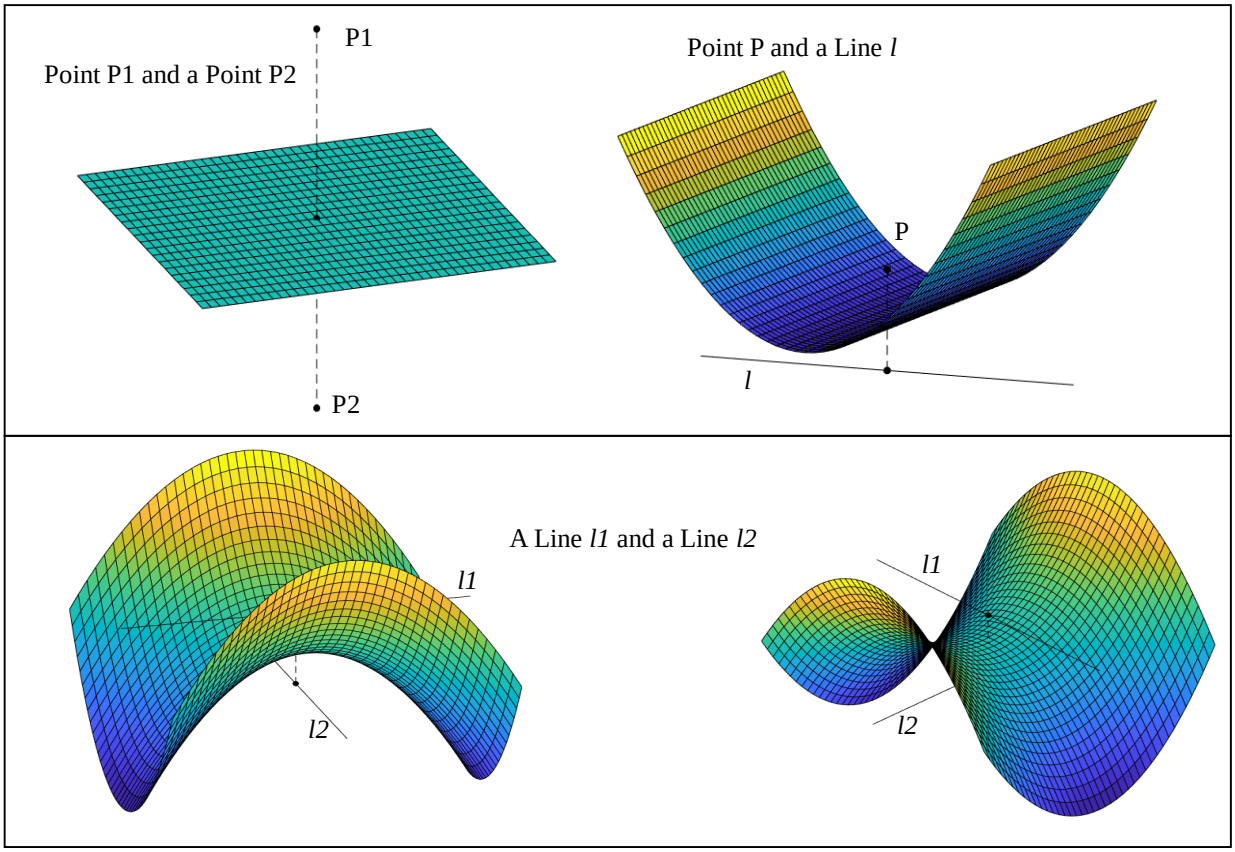

Figure 2.2: Locus of points equidistant to different combinations of points and line. (i) point and point (top left) which is basically a plane perpendicular to the line joining them. (ii) Point and Line (top right) - we get a cylindrical paraboloid with the point as the focus and the line as the directrix (iii) For a general case of two non-intersecting Skew lines (bottom two) - we get a **Hyperbolic Paraboloid** which has the famous saddle point at the middle of the closest line segment between the two line *l1* and *l2*. All these figures are created using MATLAB R2017b

have very interesting surfaces.

2.3.2 Boundaries Voronoi Regions in 3D

Voronoi diagrams can also be constructed in 3D space (or even N-D space). These result in polyhedral cells in higher dimensions. The boundary of the Voronoi cells is basically the locus of all points that are equidistant from the two cells shared by the boundary. Figure 2.2 shows locus of equidistant points created in the 3D space for the corresponding geometric entities.

Clearly the interesting shape occurs when we have two lines in 3D. If the two lines are co-

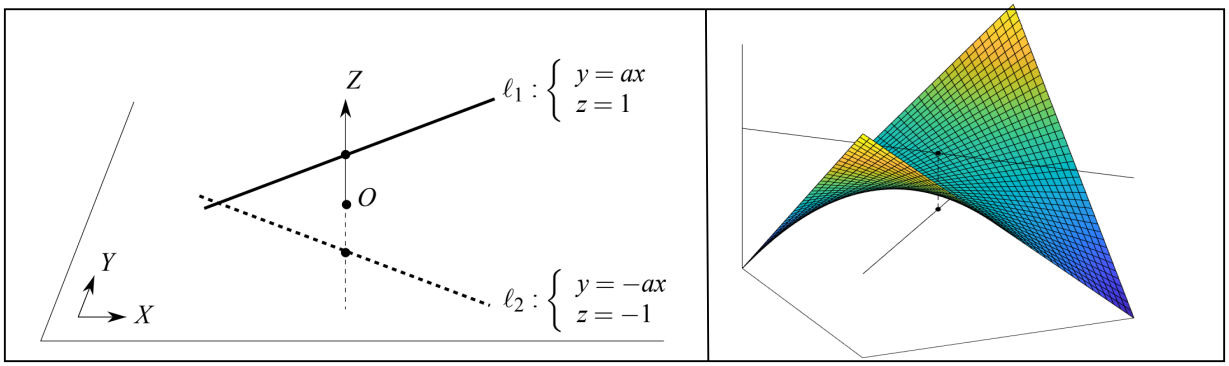

Figure 2.3: The two lines l1 and l2 assumed in a Cartesian coordinate reference and its equidistant surface shown in the right the equation of the surface is given by $Z = cXY$, where c is a constant depending on the variable 'a'. All the figures are created using MATLAB R2017b

planar and intersecting - the Voronoi surface is basically a plane that is the angle bisector of the two lines. Also, if the two lines are parallel, the Voronoi surface is a perpendicular plane to the plane containing the two line and which passes exactly through the middle of the two lines.

Now consider two non-intersecting skew lines in 3D represented by l_1 and l_2. Without loss of generality, we can transform and scale the 2 lines such that it is parallel to the x-y plane and reoriented such that the closest line segment between l_1 and l_2 is coinciding with the z-axis (Refer Figure 2.3).

The bisector of two lines l_1 and l_2 is the set of points p whose perpendicular distance is same from the the lines l_1 and l_2. Let P_1 and P_2 be the points in line l_1 and l_2 and let $\hat{n_1}$ and $\hat{n_2}$ be their corresponding normals.

Equating the square of distance from the point P to the two lines l_1 and l_2, we have

$$||(P - P_1) \times \hat{n_1}||^2 = ||(P - P_2) \times \hat{n_2}||^2 \tag{2.1}$$

where P is point (x, y, z) equidistant from the two lines.

For the lines given in Figure 2, we have $P_1 = (0, 0, 1)$ and $P_2 = (0, 0, -1)$.

The normals are $\hat{n_1} = (\frac{1}{\sqrt{1+a^2}}, \frac{a}{\sqrt{1+a^2}}, 0)$ and $\hat{n_2} = (\frac{1}{\sqrt{1+a^2}}, \frac{-a}{\sqrt{1+a^2}}, 0)$.

Substituting these in equation 2.1, we obtain,

$$\begin{vmatrix} \hat{i} & \hat{j} & \hat{k} \\ x & y & z-1 \\ 1 & a & 0 \end{vmatrix} = \begin{vmatrix} \hat{i} & \hat{j} & \hat{k} \\ x & y & z+1 \\ 1 & -a & 0 \end{vmatrix}$$

After expanding and rearranging, we will get the following equation.

$$z = -\frac{a}{1+a^2}xy \tag{2.2}$$

Equation 2.2 describe a surface that is commonly called a saddle shape. Specifically, the shape described by this equation is known as hyperbolic paraboloid which is a type of bi-linear surface. Thus, generally speaking, the locus of all points equidistant between two skew lines given in 3-space will be a right hyperbolic paraboloid. This means that we can conclude that the nature of every boundary formed in Voronoi region a set of skew lines in 3D space would is a hyperbolic paraboloid. We will use these results later in the Chapter 3 to explain how using Voronoi decomposition helps creating topologically interlocking shapes.

2.3.3 Voronoi Partitioning with Higher Dimensional Sites

It can be interesting to create the Voronoi diagram of other objects, such as lines, polygons or even polyhedra. Various people have already created algorithms for the exact Voronoi diagram of lines and areas in 2D [71]. The 3D JFA algorithm by Rong and Tan [72], is able to create a discrete 3D Voronoi diagram, however, it does this by creating several 2D Voronoi diagrams, and adding them together to form a 3D Voronoi diagram.

While there are algorithms for Voronoi decomposition of points in 3D, little is known about Voronoi of higher dimensional sites (lines, surfaces and volumes) in 3-space. A recent paper by Franz Aurenhammer et al. [73] proposes a space sweep algorithm to compute voronoi diagram for parallel half-lines at logarithmic time per face. Hazel Everett et al. devoted a separate paper to investigate the topology and studied the voronoi diagram of 3 arbitrary pair-wise skewed line

segments [74]. They also presented some algorithms for determining a rational test for querying which Voronoi cell a corresponding Voronoi site belonds to.

It is interesting to note that complex shapes from conics can be constructed simply by finding the voronoi tessellations between skewed line segments. However, the difficulty increases when we have more than 2 lines in the space. However, several subproblems derived from this has been used for wide applications. Debasish Dutta et al [75] examined a number of specific cases in which voronoi surface has a simple geometric structure. The somewhat reverse problem is to finding the set of line segments that would give a particular surface contour. This is widely known as Medial axis for any given object that is basically the set of all points having more than one closest point on the object's boundary [76].

Recently, Vladlen Koltun et al [77] showed that combinatorial complexity of Euclidean voronoi diagram of *n* lines in 3-Space that have at most *c* orientations is O($c^4 n^{2+\epsilon}$) for any given $\epsilon > 0$. He believes this is a step towards proving that the problem of solving the 3D Voronoi with line segments has a near-quadratic complexity. This conjecture has been there only for 3D Voronois with lines with Euclidean metric. The case of Vornoi based segmentation in Euclidean space is harder than Polyhedral metric (distance functions). The reason is that, in Euclidean metric the surfaces assume quadratic form and it becomes harder to calculate the intersection. Under polyhedral metric distance, a tight upper bound has been studied extensively and a tight upper bound of $O(n^2)$ has been established [78] simply by invoking the properties of involved geometric structures.

This general problem of 3D Voronoi for line segments in Euclidean Metric has also been listed as Problem 3 in the list of Open Problems Project in computational geometry, published by Mitchell and ORourke. In this work, we present two potential algorithms to obtain approximate solutions of Voronoi partitioning of line segment, curves and higher-dimensional Voronoi sites. The construction algorithm we present in Chapter 3 runs with a time complexity of $O(k\ n\ logn)$ where k varies is level of discretization of the region in-between the two planes and n is the number of Voronoi entities that we use to partition the space. The algorithm presented in Chapter 4 runs

with a time complexity of $O((k\ n)\ log(k\ n))$ where n is the number of input Voronoi sites, and k is the number of samples in every Voronoi site.

3. DELAUNAY LOFTS*

3.1 Introduction

The biological community modelled cells that packed together to form thin structures (such as organ skin) as primarily prism-like shapes (see Figure 3.1). This view was recently updated through the discovery of "scutoids" — shapes that frequently occur in animal skin-cells [2]. The formation of these thin (2.5D) structures can be viewed as a topology changing interpolation through edge-collapse or vertex-split operations between quadrilaterals, pentagons and hexagonal faces of any given tessellation.

Inspired by this new discovery, we first offer a view that provides a *dual* version of this explanation. We observe that scutoids could be formed by a Voronoi partitioning of a shell into regions based on distance to a set curves along the thickness of the shell. This dual explanation is theoretically useful since (1) it provides a well-defined process to compute the boundaries of resulting structures; and (2) it is able to naturally create curved boundaries that is expected for resulting structures.

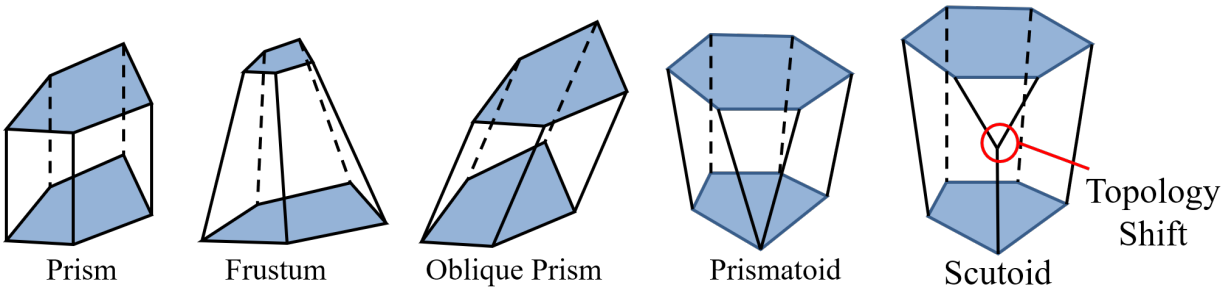

Figure 3.1: Difference between prism-like shapes and Scutoid. The highlighted topology shift in the middle of the two faces is what makes Scutoids different from others. The skin cells are typically modelled using prism structures. And the bending of skin cells are usually explained modelling cells as frustums.

*Part of the data reported in this chapter is reprinted with permission from "Delaunay Lofts: A Biologically Inspired Approach for Modeling Space Filling Modular Structures" by Sai Ganesh Subramanian, Mathew Eng, Vinayak R. Krishnamurthy, Ergun Akleman, 2018. *Computers & Graphics*, 82, Page range 73-83 including figures 3.2, 3.4, 3.6, 3.10, 3.11, 3.12, 3.14 and 3.15

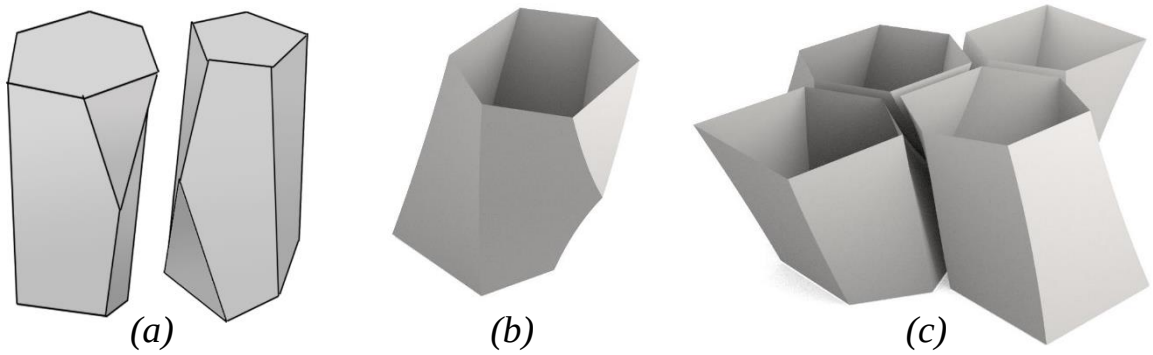

Figure 3.2: A comparison of the original scutoid discovered by Gomel-Gomez et al. [2] (a) with the one generated by our method (b) shows the difference between the interfacing boundaries between two different blocks. Note that not more than 4 of these shapes can be fit together which means these structures are not repeatable and cannot fill the space (c). The shapes generated using our design method are repeatable and fill the 3D space.

From the shape modeling point of view, this dual explanation provides a simple yet powerful conceptual framework that can be used to model and design a wide variety of modular shell structures. Users can simply provide *a set of control curves as Voronoi sites to obtain a decomposition of a thin plate*. Even straight lines can result in interesting structures with curved boundaries. Based on this explanation, we have developed a set of simple and intuitive procedures to design a wide variety of unconventional — and also non-intuitive — building blocks.

Figures 3.4 and 3.11 show examples of such non-intuitive space filling tiles that are designed using our procedure. In Figure 3.4, one way to reason regarding the extremal tilings is to view the bottom layer as a translated version of regular square grid in the top layer. Sweeping of a square profile through translation is normally expected to result in a prism with planar parallelogram faces. However, tilings are not standard single objects. We can obtain a rigid body transformation of a tiling in more than one way. Figure 3.4(b) shows how the tiling is interpolated in this particular case.

As it can be seen in Figure 3.4(b), the motion of Voronoi sites produces hexagonal grids, which causes a change of 1D topology from quadrilateral to hexagon and back to quadrilateral. This topological change is clearly visible in the 2.5D tilings shown in Figure 3.4 by triangles resulting

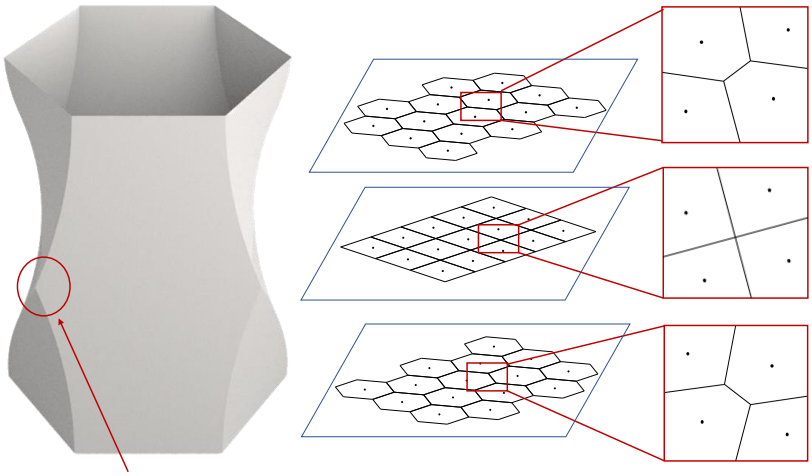

Figure 3.3: Figure showing topology shift happening in a Delaunay Loft. This representations shows a transition of a 3-Valency Voronoi vertex in the middle layer to 4-valency Voronoi vertex and vice versa.

from edge collapse — a change that is also noted by the researches on biological cell packing [2]. Further, note that these triangles are not planar since they are naturally created as a by-product of Voronoi decomposition. Since the top and bottom tilings are rigid transformation of each other, these are 3D space filling shapes as shown in Figures 3.4 and 3.11.

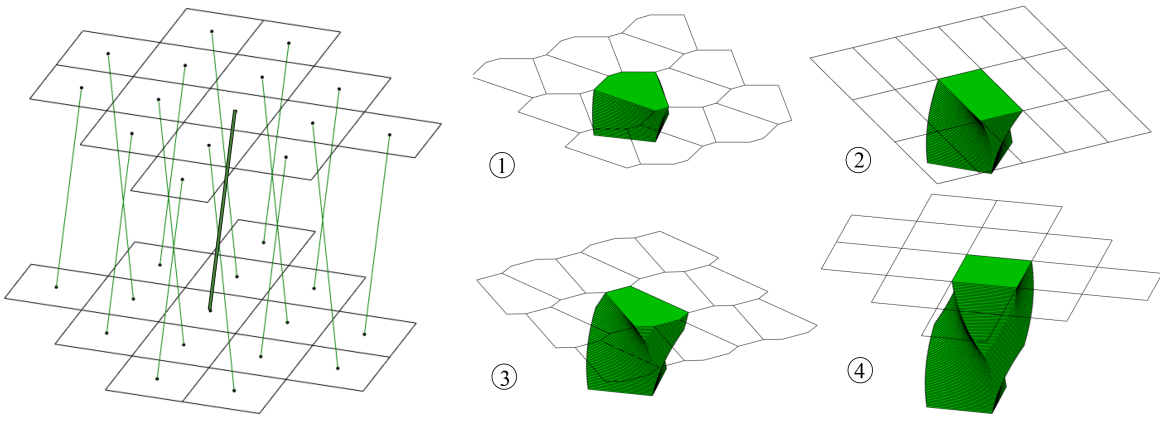

Figure 3.4: The process of construction of Delaunay Lofts. We first creates a set of control curves shown on the left. Note that the control curves that interpolates Voronoi sites are shown in green and the Voronoi sites are black dots. The construction of Delaunay Lofts is demonstrated in a four step process as shown in the right.

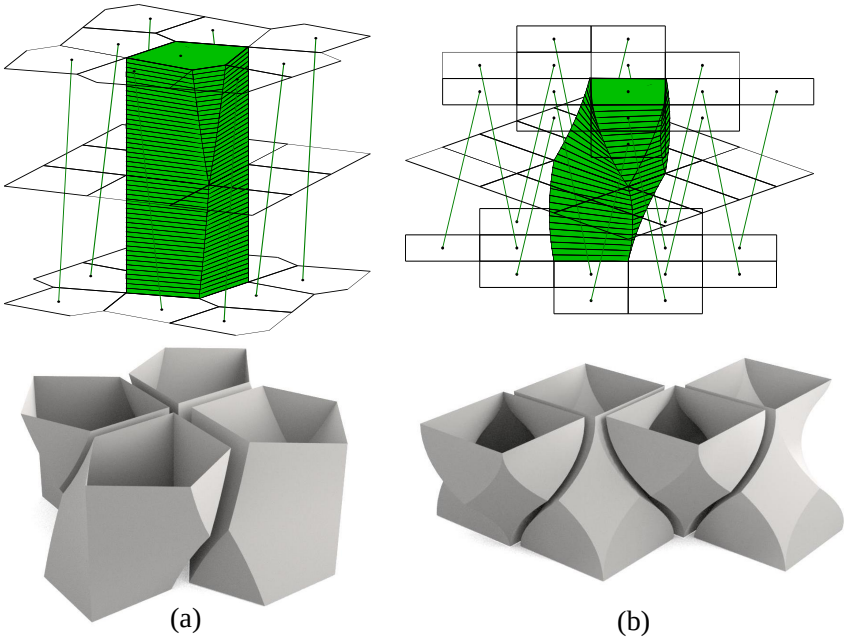

(a) (b)

Figure 3.5: (a) Pentagonal Delaunay Lofts — this is got by interpolating between two regular pentagonal tiling with a quad layer in the middle (b) Quad Delaunay Lofts — interpolation between three different quad layers.

3.2 Mathematical Foundations

In this section, we provide the basic foundations for our approach. All the information in this section is well-known. We only provide it to establish a context for our approach. This background will provide a foundation for the development of algorithms to construct space-filling tiles in 3D space.

3.2.1 Fundamental Domain

In this paper, we present our approach as the decomposition of a 3-torus that is given as a repeated cubical domain, $[0,1]^3$ [79] as its fundamental domain. In other words, $x \equiv x - \lfloor x \rfloor$, $y \equiv y - \lfloor y \rfloor$, and $z \equiv z - \lfloor z \rfloor$ where the floor operator ($\lfloor a \rfloor$) gives the greater integer less than or equal to a. This gives us a regular tessellation of 3D space. We usually assume that z does not repeat and $0 \leq z \leq 1$ represents a shell, i.e. a 2.5D structure. We further assume that curved shapes are obtained by a deformation of this domain such as a tensor product free-form volume that

is defined on this cubical domain [80, 81]. Such deformations are, of course, not straightforward, but we purposely provide our presentation using this simple domain to simplify our explanation without loss of generality.

3.2.1.1 Domain Decomposition using Control Curves

Given the fundamental domain, our approach is simply to compute a Voronoi decomposition of this cubical domain into the regions based on distance to a set of curves given in the form of $(x_i = f_{i,x}(z), y_i = f_{i,y}(z))$, where $i = 0, 1\ldots,$ n. Since these curves intersect any given $z = c$ constant plane only once, with a well-defined distance function, the decomposition of the 3D domain can be simplified as a sequence of 2D Voronoi decomposition at each planar layer, $z = c$, based on the distance to a set of points $(x_i = f_{i,x}(c), y_i = f_{i,y}(c))$ (See subsection 3.2.2).

3.2.1.2 Interpolation Curves

We further assume that each of these control curves are interpolations of a set of control points given $z = c_j$ as $(x_{i,j}, y_{i,j}, c_j)$. We simply choose these points to obtain any desired Voronoi decomposition in any given planar layer. Using these points as control points of the curves we can obtain any desired Voronoi decomposition. For interpolation, there is really no preference. We can even simply use piece-wise linear interpolation.

3.2.2 Distance Functions

We observe that scutoids could be viewed as shapes constructed from 2D Voronoi diagrams that are stacked on top of each other. The shapes of the scutoids result from changes of the polygonal topology of the 2D Voronoi diagrams as we move along each interpolated plane ($z = c$). In particular, edges of Voronoi cell polygons in different layers either collapse or split by changing vertex valences. To formalize this observation, we need to show that there actually exists a formal distance function that can produce such layer by layer 2D Voronoi diagrams. In this part, we demonstrate that this distance function actually exists.

3.2.2.1 Generalized Distance Function

Let $\mathbf{v}$ be a vector between two points and $L_m(\mathbf{v})$ be any linear function with $m = 0, 1, \ldots, M-1$. It has been shown that the following generalization of Minkowski distance functions can be used to compute distance between any two points [82]:

$$d(\mathbf{v}) = \left(\sum_{m=0}^{M-1} ||L_m(\mathbf{v})||^p \right)^{\frac{1}{p}} \tag{3.1}$$

where M is the number linear functions. To simplify the discussion, we assume that the linear function L_i takes the form:

$$L_i(\mathbf{v}) = \frac{\mathbf{n_m} \cdot \mathbf{v}}{s_m} \tag{3.2}$$

Here, $\mathbf{n_m}$ is a unit vector and $s_m > 0$.

3.2.2.2 Circular Disk Distance Function

Let us now consider a specific distance function in 3D where $L_0(\mathbf{v}) = x$, $L_1(\mathbf{v}) = y$, $L_2(\mathbf{v}) = z/s$, and $p = 2$, which gives us

$$d(x, y, z) = \lim_{s \to 0} \sqrt{x^2 + y^2 + \frac{z^2}{s^2}} \tag{3.3}$$

In this case, the implicit shape $d(x, y, z) = 1$ is an ellipsoid that will ultimately go to an infinitely thin circular disk as s tends to zero. Unfortunately, $s = 0$ will not lead to a valid distance function since $d(0, 0, 0)$ must be zero for a norm and z/s is undefined when both z and s are zero. On the other hand, if s is arbitrarily close to zero, z/s is still zero when $z = 0$.

An important interpretation of this circular disk distance is that any two points in the same layer are closer to each other than to points in layers above or below s amount since $d(0, 0, z) > d(x, y, 0)$ for $(x, y) \in [0, 1]^2$ and $|z| > s$. This is a big advantage since we now can reduce the problem of searching for equidistant boundaries in thin rectangular layers bounded by s in z and 0 and 1 in x and y. Assume that the domain consists of N layers in z direction and $s = 1/N$. Then,

every layer will be given by an implicit equality as $is \geq z \geq (i+1)s$ with $i = 0, 1, \ldots, N-1$. We also assume that the intersection of each curve with any given layer will always be confined by a circle with radius $\sqrt{2}s$. This can easily be obtained by choosing the tangent direction never makes more than 45^0 with z direction. We also assume that highest frequency of the control curves never exceeds Nyquist limit [83]. Then, we can safely sample the curves at $z = s(k+0.5)$ to use $x_i = f_{i,x}(s(k+0.5)), y_i = f_{i,y}(s(k+0.5))$ as 2D Voronoi sites and we can view this decomposition as a discretization of the cubical domain into N number of 2D domains given as $z = s(k+0.5)$.

In other words, under the assumption that the 3D structure is *thin* (as characterized by the discussion above), the 3D Voronoi decomposition reduces to 2D Voronoi decomposition of points. These assumptions can be safely imposed in a scenario where a user is designing the interpolating curves and the number of samples. This distance function significantly simplifies especially the construction of the resulting 3D shapes by converting the computation of 3D Voronoi decomposition of lines into 2D Voronoi composition of points. Based on this distance function, the construction can be done in real time during interactive design. In order to develop an intuitive design methodology for shape design, we use Delaunay diagrams.

3.2.3 Delaunay Diagram

It has been shown that the computation of a Voronoi diagram can be greatly simplified by working with its dual, which is known as the Delaunay diagram of the given sites [84, 85, 86]. Figure 3.6 shows the construction of a Voronoi diagram using the Delaunay diagram. Delaunay diagrams also turn out to be useful for designing the proposed Delaunay Lofts since the problem of interpolations of polygons simplifies into that of merely interpolating points along a set of control curves. With Delaunay diagrams we can precisely design the control curve as an interpolation curve that goes through a set of critical points that defines exact locations where the polygonal topology changes.

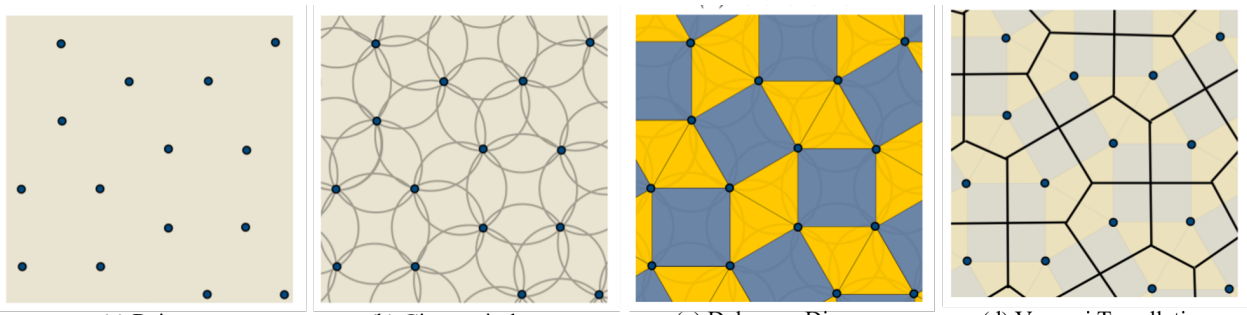

(a) Points (b) Circumcircles (c) Delaunay Diagram (d) Voronoi Tessellation

Figure 3.6: An example to demonstrate how to design single polygon tilings as dual meshes of regular or semi-regular tilings. Note that each polygon in semi-regular Delaunay diagram is regular, and therefore, cyclic. (c) shows a Delaunay diagram that is a semi-regular mesh with the same vertex figure, which is $3.4.3.4.3$. The corresponding Voronoi Diagram in (d) is a tiling that consists of the same polygons, which are pentagons. This property holds for all semi-regular tilings.

3.2.3.1 Cyclic Polygons

The key idea behind Delaunay diagram are cyclic polygons. To precisely control polygonal topology changes, we use the fact that when n-number of points forms are inscribed in a circle, they form a convex cyclical polygon and their n-perpendicular bisectors to the sides are always concurrent and the common point is always the center of the circle (Figure 3.6(b)). This property helps us to design desired control curves by directly controlling the number of sides and vertex valances of a Voronoi tessellation in every layer. We basically create the desired Delaunay diagrams in some layers and interpolate their vertex positions. The only issue is to keep the number of vertices identical.

3.2.3.2 Diagram vs. Triangulation

We want to point out that Delaunay diagrams are not exactly Delaunay triangulations. Specifically, a triangulation of $n \geq 2$ sites is Delaunay if and only if the circumcircle of every interior triangle is point-free [86]. One well-known but misleading property of Delaunay triangulations is that when four or more points are on the same circle, we can still create a formal Delaunay triangulation by triangulating these faces since any of these non-unique triangulations still satisfy the two properties of Delaunay triangulations. Delaunay diagrams are the real dual structures of Voronoi

diagrams wherein a face becomes a vertex and a vertex becomes a face (Figures 3.6(c) and 3.6(d)).

In a Delaunay diagram, we draw only one polygon per unique circle. Not only does this eliminate any ambiguity but also simplifies the design process since the number of sides of the polygon directly defines the valence of corresponding Voronoi vertex. In the rest of this section, we discuss a few strategies to design Delaunay triangulations.

An important implication of this observation is explicit controlling topology changes. In a Delaunay triangulation, if more than one triangle share the same circle, the corresponding triangulation is not unique since it means more than three Delaunay vertices form a cyclic polygon. The number of vertices of these cyclic polygons directly determines the valance of corresponding vertex in Voronoi structure. Therefore, by controlling how many triangles share the same circle in every layer, we can change mesh topology in any desired layer.

3.3 Contruction Methodology

Here, we describe the algorithm to create Delaunay lofts. The important aspect of the algorithm is to achieve vertex-split and edge-collapse operations that occurs during the topology shift (Figure 3.3).

3.3.1 Pre-processing input line segments

1. Obtain the input line segments between two layers.
2. Sample a number of layers between these two extreme layers
3. Now for every layer i between 0 to $n-1$ where n is the number of layers
4. Find the Voronoi Decomposition of the points we get intersecting the line segments with the layers i and layer $i+1$
5. For a given line find the two Voronoi cells in layer i and $i+1$ and evaluate the side boundary faces

Note that the two voronoi polygons may have different number of vertices and edges. We are looking some sort of mapping between the two polygons.

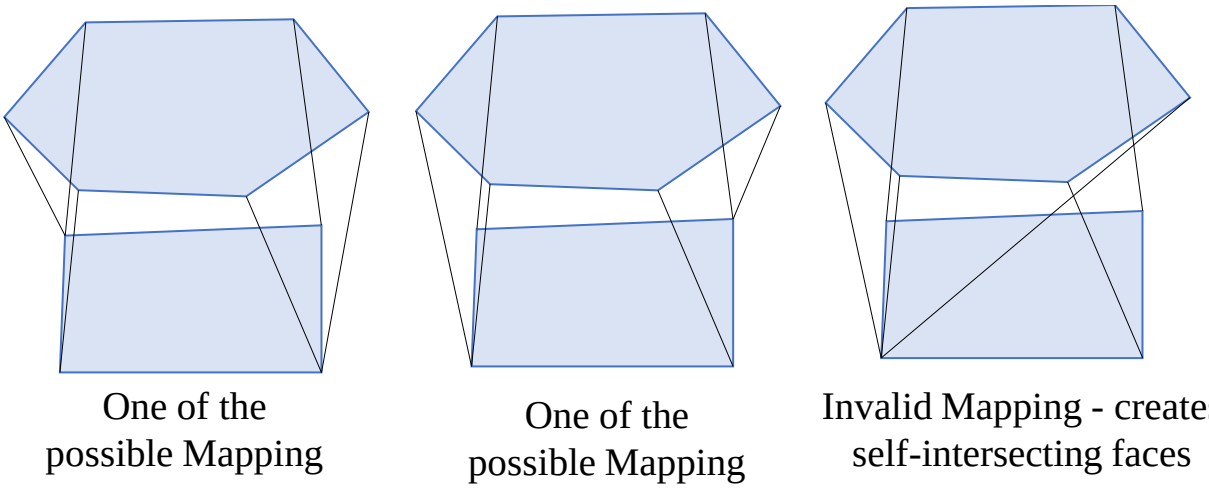

Figure 3.7: Possible mapping between two polygonal faces out of which some result in self-intersecting shapes.

3.3.2 Finding the Side boundary faces

Assume two polygons of sides M and N. We basically need a way to connect the vertices of one polygon to the other polygon to construct the side faces of the loft. Out of all the possible mappings of vertices, there are several valid and several invalid mappings. Invalid configurations are those that gives us non-manifold edges and surfaces — our algorithm should not give raise to these shapes (Figure 3.7). And out of the valid configuration, there exists only one mapping that creates the right faces. We find that configuration using the following steps.

1. First find the closest two pairs of vertices between the two polygons.

2. Assuming these two points as reference, assign two parameters u and v ranging from $[0, 1]$ along the perimeter of the each polygon which serves as the parametric position to each corner of the cell.

3. Then follow the pseudo-code to insert the edges between the vertices.

This method can also be extended to create lofts with curved control lines — this allows for a wider range of tilings in the design space.

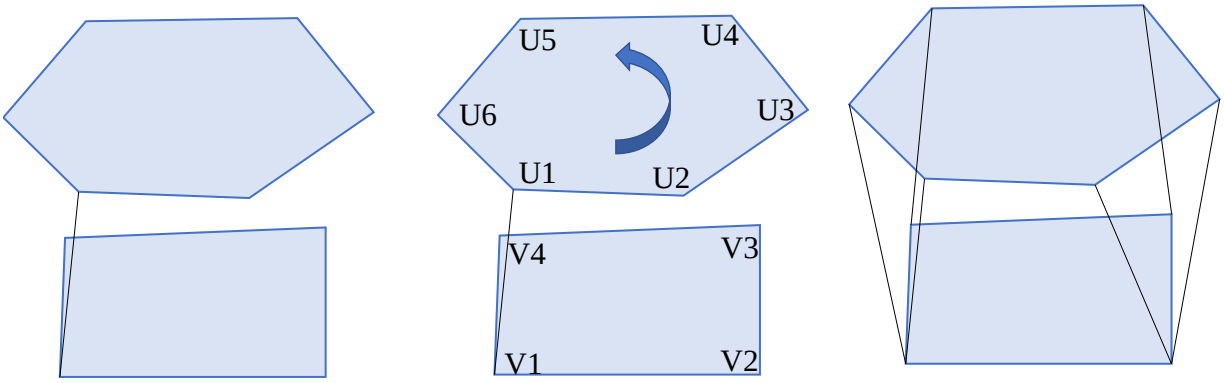

First edge inserted between the two closest vertices

Parameterize the polygons

After iteratively adding the edges using our algorithm

Figure 3.8: The algorithm for creating the shape of a single Delaunay Loft in parameter domain.

Algorithm 1: Pseudocode for Single Delaunay Loft

```
n = 0; m = 0;
while (n ≤ N and m < M) or (n < N and m ≤ M) do
    if (n <N) then
        n = n++;
    if (|u_n − v_m| ≤ |u_n − v_{m+1}|) then
        InsertEdge(u_n, v_m);
    else
        InsertEdge(u_n, v_{m+1});
        if (m <M) then
            m++;
```

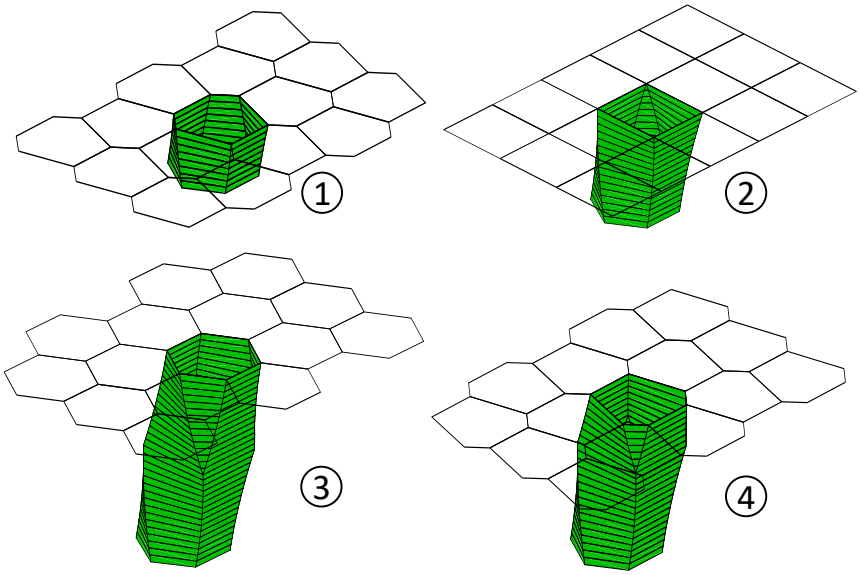

Figure 3.9: Status of the generated shape at different stages of algorithm for a Delaunay Loft.

3.3.3 A Note on Time complexity

Given *n* line segments, the time complexity of the algorithm is dependent on the number of layers we discretize the line segments into. Let us assume we divide the region into *D* equidistant layer. Now, the algorithm with the best time complexity that we can use to obtain the voronoi decomposition of any 2D layer is O($n\ logn$) (Fortune's algorithm for example). This Voronoi computation is repeated in every layers (assume 'd' number of layers). Thus, the overall combinatorial time complexity of this approach would be O($d\ n\ logn$).

3.4 Designing Control Lines

3.4.1 Based on Quad Layer

The topology shift that makes Scutoids interesting (see Figure 3.1 happens when a voronoi edge that gets collapsed to a four-valency vertex and then splits back into an edge. We saw that how this happens automatically if we use Voronoi partitioning in every layer. However, we do not yet have a control where the topology is changing since it is primarily dependent on the Voronoi polygons on the top and bottom that we are interpolating. So, one of the methods to get control

over the topology shift is that if we arrange points in rectangular grid, the Voronoi decomposition will automatically create Voronoi vertices with four valency. So if we enforce the line segments to pass through a quad layer in the middle, the topology shift is ensured to happen in that layer.

3.4.2 Based on Wallpaper Patterns

In order to get repeating tiles we need the point distribution in every layer to adhere to some sort of symmetry or pattern. There exist seventeen distinct symmetries in 2D plane, called wallpaper patterns. In literature, these periodic symmetry groups are called as *p1, p2, p4, pm, pmm, p4m, p4m, cm, cmm, pg, pmg, pgg, p4g, p3, p6, p3m1, p31m* and *p6m* [87]. Each one of these symmetry groups is a collection of isometric operations, which preserve the distance of any two points, i.e. translation, rotation, reflection and glide reflection. The rotations can have periods two, three, four or six. The complete list of the 17 symmetry groups in plane can be classified in two categories: rectangular and hexagonal. Namely, 12 of these 17 groups have rectangular symmetries, i.e. their natural fundamental domain is a rectangle. The remaining 5 have hexagonal symmetries, i.e. their natural fundamental domain is a hexagon.

It has been shown that we can use rectangle as the fundamental domain for hexagonal symmetries [3]. In other words, regardless of the symmetry group, any symmetric tiles can be represented by a simple rectangular fundamental domain, which can be embedded over a toroidal surface. Thus, we can construct any wallpaper by symmetry operations that is constrained in fundamental domain.

This property is not just practically useful for our application, it also provides the theoretical support to use cubical fundamental domain for Delaunay Lofts. Because of this property, we can obtain any 2D wallpaper symmetrical Voronoi decomposition that can be obtained using points as Voronoi sites in any layer. Control curves can simply be obtained by interpolating Voronoi sites (i.e. Delaunay vertices).

Another important property of wallpaper patterns, which we use, is that all semi-regular tilings can be constructed using wallpaper symmetry operations. In a semi-regular tiling the vertices being "the same" means that for every pair of vertices there is a symmetry operation. For instance, in

semi-regular mesh $3.4.3.4.3$ has the wallpaper symmetry *p4g*.

The only caveat in this approach in terms of the design is that the number of Voronoi sites in every layer has to be the same. Using a rectangle as our regular domain also provides a solution to that problem. Note that the regular rectangular domain in Figure 3.10 actually consists of two hexagons, one full (blue), and a second one that is decomposed into four pentagons (two yellow and two red). This means that if we create points in hexagonal symmetry, we need to multiply the number of points by two. Also note that the symmetries always have periods of either two, three, four or six. Using this information, we obtain the same number of points using their least common multiples (LCM). For instance, if we want to connect symmetries with four or six, 12 points will be sufficient. One will be created as three random points with four period. Another will be created as one random point with period six in two hexagons. Some of the symmetry patterns in 2D were also inspired from Kaplan's work on Ornamental design using Voronoi diagram [67].

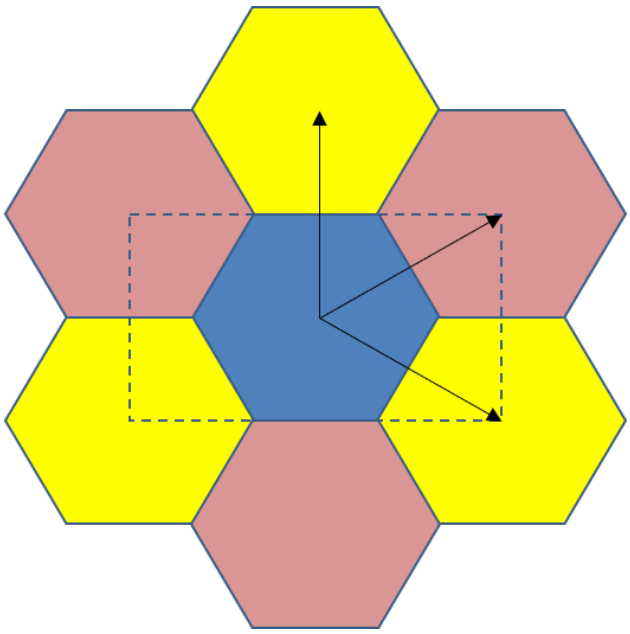

Figure 3.10: Rectangle can also be used as a fundamental domain for the five wallpaper symmetries whose natural fundamental domain is a regular hexagon [3].

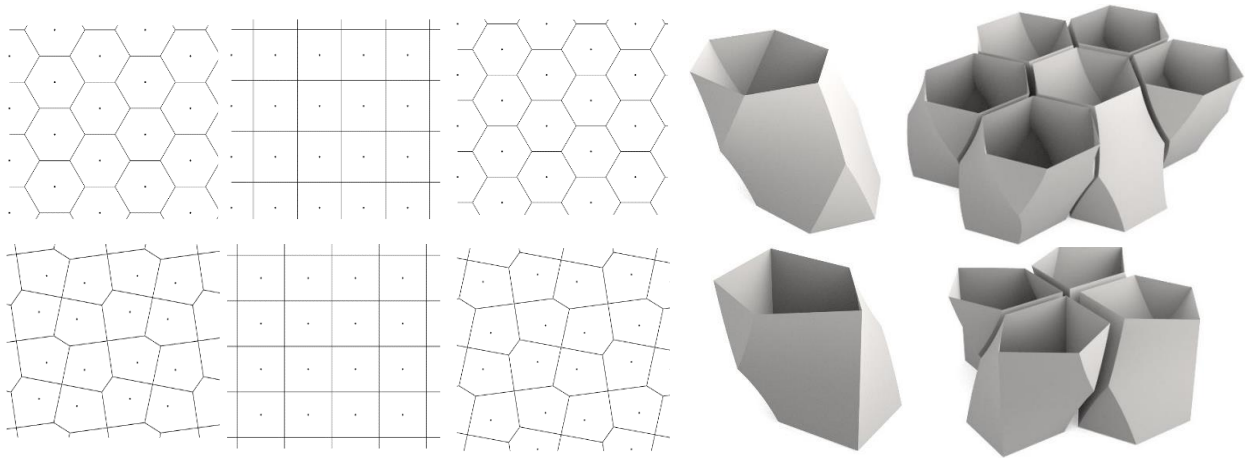

Figure 3.11: The three patterns (left to right) show the Voronoi diagrams from the bottom, middle and the top layer of interpolation. In the first row we show the 464 Delaunay Lofts and second row shows the Delaunay Lofts obtained by interpolating $3.4.3.4.3$ patterns.

3.5 Results of Delaunay Lofts

The construction algorithm allows for exploring and investigating a vast variety of shapes that are possible now. The only constraint is to have the total number of points to be equal in the two layers we intend to interpolate. To ensure repeatability of the Delaunay Lofts, we should have geometric regularity in the tilings we interpolate. In the following sub-sections, we explore different strategies for achieving the geometric regularities. Furthermore, for a few selective cases, we also conducted preliminary finite element analysis (FEA) to better understand the potential advantages of Delaunay Lofts over prisms.

3.5.1 Delaunay Lofts of Scutoids

Our approach when applied to the original scutoid discovered by Gomel-Gomez et al. (mapping Hexagon to Pentagon) [2] produces curved surfaces which is different from the common description of scutoids with planar surfaces (Figure 3.2). In our approach, the interface between any two shapes are naturally curved due to Voronoi-based interpolation ensuring that the tiling is space-filling. The important this to note is that not more than 4 of these shapes can fit together to create a repeatable block. We shall now explore shapes that are space-filling.

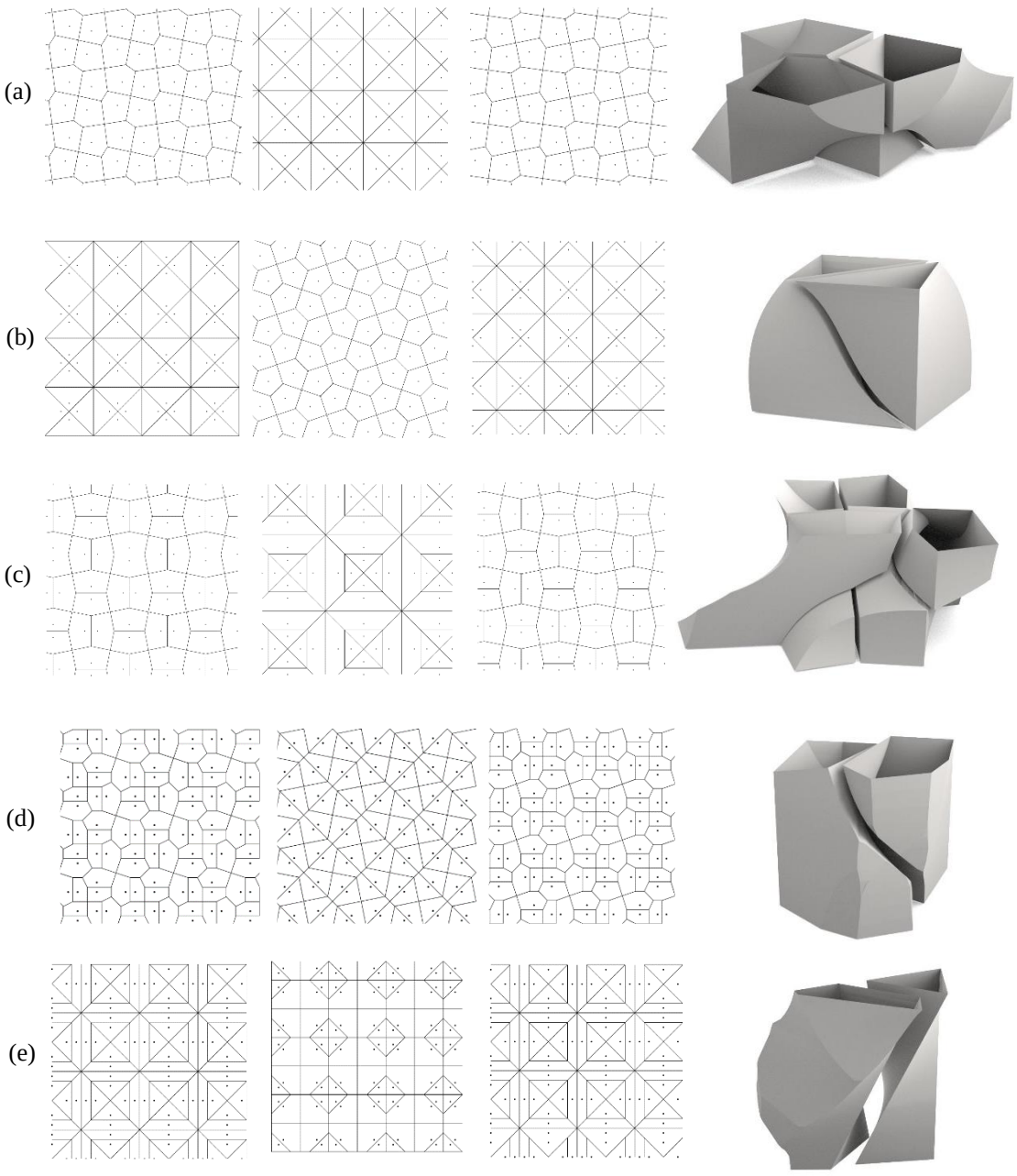

Figure 3.12: This figure shows five more Delaunay Lofts got by applying wallpaper symmetry patterns to the control curves in 3D. In each row, we show the transition of Voronoi from the bottom layer, middle layer and the top layer followed by the corresponding tiling we get. We specifically leave small gaps between the Delaunay Lofts to appreciate how nicely the shape fit well with each other. Figure (a) shows a transition from Pentagon in the Top and bottom layer with a Triangle in the middle. (b) shows Triangle on top and bottom with a Pentagonal Middle layer. The Delaunay Lofts (c), (d) and (e) however go through a series of transitions within Triangle, Quadrilateral and Pentagonal layers. This is the reason for the intricate shapes of these Lofts.

Hexagonal Delaunay Lofts | Quad Delaunay Lofts | Pentagonal Delaunay Lofts

Figure 3.13: 3D Prints of the three types of Delaunay lofts with quad layer in the middle. Notice the bifurcation that happens mid way between the top and bottom planes. We have printed an hollow version of pentagonal lofts to show the inner surface contour.

3.5.2 Delaunay Lofts with Quad Layer

Since any regular polygon is also a cyclic polygon, we start with regular polygon tilings as they are good candidates to design Delaunay diagrams. We will then extend and generalize this idea to Semi-regular and Regular tilings with Wallpaper patterns. We start our exploration with a simple Hexagonal tiling, which is one of the three Euclidean tilings of the space (apart from square and triangle). With the longer axis of the hexagon aligned vertically, we move alternate rows of hexagon tiling in opposite directions. We displace the Hexagon by an amount equal to half the horizontal distance between two subsequent cells in a row. Half way through the process, every hexagon changes to a quadrilateral. Similar interpolation pattern was also suggested by Kaplan [67] in his work on Voronoi Diagrams and ornamental design.

3.5.3 Delaunay Lofts with without the enforced Quad layer

Although we have enforced the importance of quad layer to generate Delaunay lofts with ensured topology shift, we can remove the constraint to explore symmetries based on interpolating one of the 17 wallpaper groups. We start with $p4$ symmetries wherein we take a subdivide a unit square into 4 equal square pieces and sample points with 4 rotational symmetry. By extending this symmetry to the control curves in 3D space (achieved simply by mirroring the selected control curves about the z direction), we can simply repeat the unit domain in 3D space to construct the

tilings. Most of the Delaunay Lofts we get using these symmetry patterns have highly curved interfacing between two adjacent tiles and may offer better interlocking capabilities when compared with its prism counterparts. We can also extend the tilings to semi-regular tilings. Figure 3.12 shows a number of results with the interpolation between different patterns (apart from quad grid) that we obtain from wallpaper symmetry.

3.5.4 Delaunay Lofts with Non-linear Curved Control lines

Extending our method to non-linear control curves, such as circular, cosine, or Hermitian, is especially promising for creating more unusual free-form tilable shapes. We specifically experimented with Hermitian interpolation (Figure 3.14) since it is possible to extend this to multiple control layers and more control in derivatives. Note that we do not have to be careful to keep the curves in the rectangular prism domain since the curves are conceptually drawn in 3-torus.

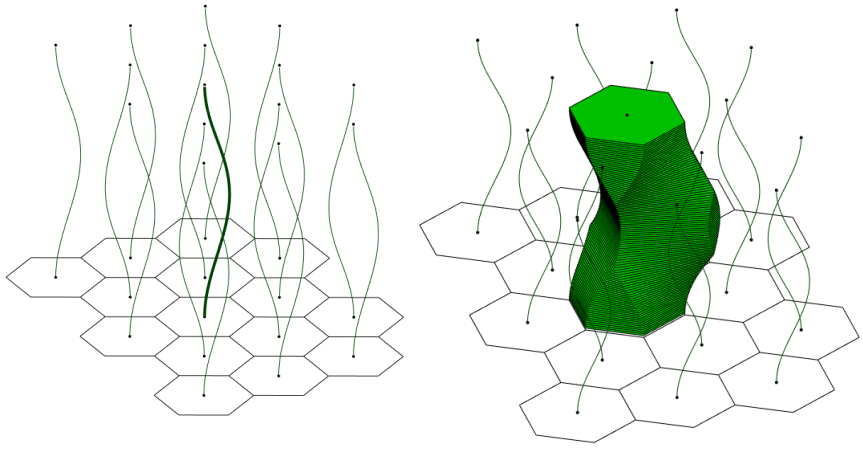

Figure 3.14: A space filling Delaunay Loft obtained by Hermitian curves.

3.6 FEA on individual Delaunay Lofts

We conducted a preliminary FEA on the 464 Delaunay Loft with the hypothesis that since the central layer ($z = 0.5$ in parametric domain) is enforced to be a regular quadrilateral tiling, we will observe some interesting effects at this layer when compression, tension and torsion are applied in-

dividually to a single 464-Loft (Figure 3.15). This indeed turned out to be true. The analysis shows that the stress levels are lower in the regions where the topology changes (vertex-split and edge-collapse occurs). We suspect that these mechanical properties are likely as scutoids are proved to stabilize the three-dimensional packing and minimize the tissue-energy based on biophysical arguments as proposed by Gomel-Gomez et al [2]. A detailed and systematic investigation is needed to confirm this hypothesis.

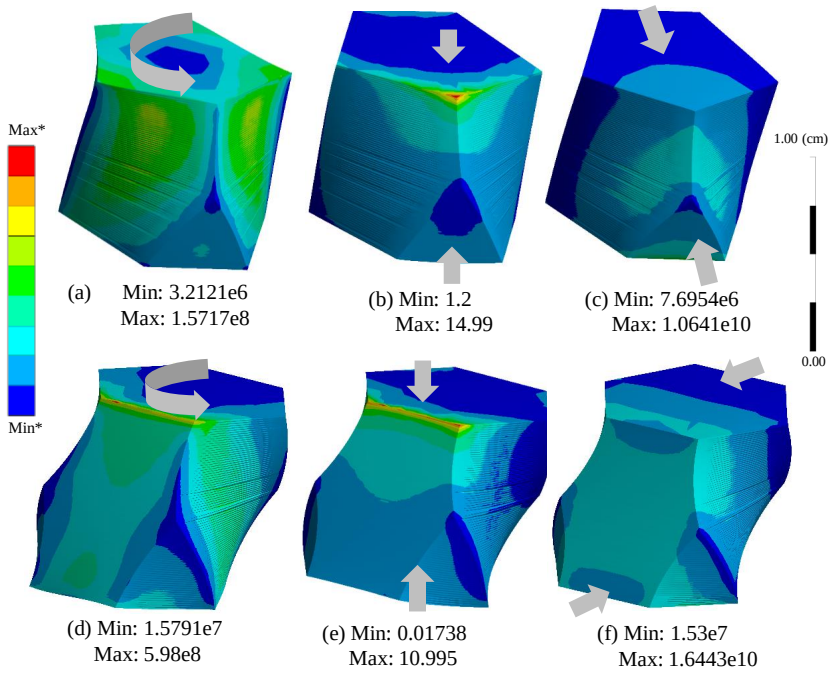

Figure 3.15: Contour-Maps of Equivalent Stress (von-Mises) of two Delaunay Lofts (Pent-Quad-Pent on top row, Hex-Quad-Hex on bottom row) are shown for three loading conditions, namely, torsion (a, d), compression (b, e), and shear (c, f). In all cases, the stress distribution decreases around the critical points where the topology changes. The torque and compression stress were 1 Nm and 1 Pa respectively. The Lofts were sheared by displacing the top layer by 0.1 mm with a fixed bottom layer. All simulations were done using ANSYS 2019 R1.

3.7 Topological Interlocking in DL

From the shape and packing of Delaunay Lofts, we notice a potential for Topological Interlocking. This is mainly because some faces of Delaunay Lofts are curves that resembles the concavo-convex contact surfaces of an Osteomorphic block (see Section 2.1.1). Thus, we seek to study the extent of topological interlocking for different shapes of Delaunay Lofts. The hope is that this will lead us to a generalized methodology for designing control curves whose shapes are ensured to be topologically interlocking.

3.7.1 Evaluation Methodology

We create assemblies of individual shapes where the peripheral tiles are fixed. We displace the central tile of the plane by $1e-4$ mm uniformly across all the simulations. Specifically the values of stress and strain are observed for different assemblies. All the analysis were static structural and was performed in ANSYS Workbench 2019 R1. The simulations were done using a PLA material to base our understanding with the 3D prints. All contacts were made friction-less because we wanted to see the effect purely due to Topological interlocking.

3.7.2 Interlocking in Hexagonal Delaunay Lofts

We created an 8x8 assembly of the Hexagonal Delaunay Lofts and performed the simulation under the conditions mentioned in Section 3.7.1 (see figure 3.16). We expected this simulation to converge to a solution where the displaced tile would distribute the stress around the contacting tiles. However, to our surprise we found that the solution failed to converge. This means that there are some sliding contacts in the solution and simply fixing the peripheral tiles does not ensure that the tiles are topologically interlocking.

Subsequently, we tried running a smaller 3x3 version of the hexagonal assembly where there is a lower possibility of sliding due to reduced number of blocks. We found that the stress propagates to all blocks around, except for one (see figure 3.17). Notice this happens because, in the assembly the block with zero stress induced is directly below the block that is displaced, thus not transferring

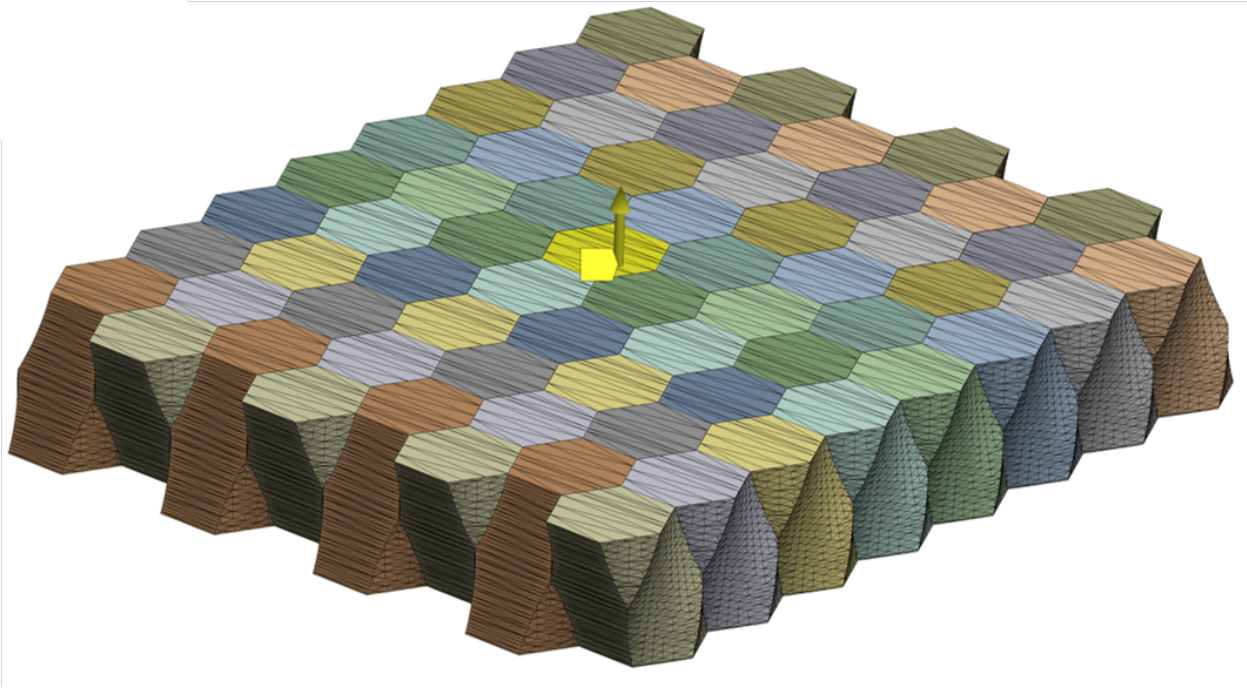

Figure 3.16: This is the 8x8 assembly of hexagonal Delaunay loft that was used for simulation. The yellow arrow in the middle tile highlights the direction of out of plane displacement given to the individual face. This simulated failed to converged to a solution.

the force or stress across. This suggests that the existence of planar surfaces in the shape of the repeating shape potentially causes lack of transfer for forces in one direction. So, *if a planar face is shared by two blocks in an assembly, the resistance will only be offered if the tile removed is below the adjacent tile. In other words, the component of normal force from the block on the other side of the planar face should be downwards to transfer the forces across.* This shows that planar faces transfer the forces only unidirectionally.

From section 2.3.2 we note that if we any two co-planar line segment, we will get a planar face. In the case of hexagonal Delaunay Loft, the lines that belong to the same row are parallel and are thus co-planar. We believe that two non-intersecting lines that create a bilinear surface (that are curved in both directions) are important for creating interlocking shapes. In fact, it can be clearly seen from the simulation results (see Figure 3.17) that the stress is easily transferred across. To further validate this idea, we performed simulation for pentagonal Delaunay lofts.

3.7.3 Interlocking in Pentagonal Delauany Lofts

The control lines that define a pentagonal Delaunay loft is non co-planar. So, based on our observation made with the simulation of hexagonal Delaunay lofts, we can expect that the simulation of displacing a tile in a pentagonal assembly would converge to a solution since the surface contacts are curved and it would distributes the forces across the assembly. The simulation results did show that the pentagonal lofts converged to a solution supporting our hypothesis that bi-linear surfaces create allow for increased interlocking.

This intuition is also mathematically validated. Bilinear surfaces — the type of surface that we obtain between two skewed line segments (see 2.3.2) — are known to have negative non-zero Gaussian curvature . This means that at any point in the contact surface between the two blocks, we will have two curvatures that are opposing each other. We believe a rigorous mathematical analysis of the force applied by the contacting surfaces and its effect in the block may lead to a general theory of creating Topologically interlocking space-filling shapes.

3.7.4 Grouping

By carefully choosing the lofts that we want to group, we can combine more than one tiles which can together fill space. We found that this has the potential to augment interlocking capabilities of the individual lofts. We considered the hexagonal Delaunay loft and combined two adjacent shapes together. FEA shows that the lack of stress propagation in one direction of the assembly in the 3x3 simualtion (figure 3.17) here is overcome by the stress induced by the adjacent hexagonal loft joint together. See figure 3.19 for the result of the FEA simulation. Note that the simulation converges and the stress propagates all the way to the boundary.

3.8 Summary of Delaunay Lofts

3.8.1 Geometric Properties & Tilings

Broadly speaking, there are two main geometric requirements that was needed from the 3D shapes that we intended to create. First, we wanted to be able to compose water-tight shapes. Second, we hoped for the pattern to be composed of ideally a single (or at least a finite set of)

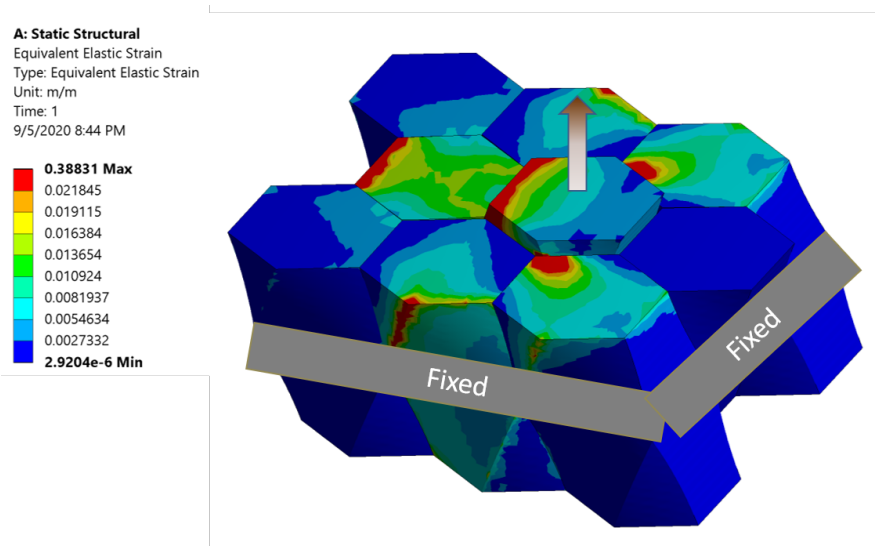

Figure 3.17: 8x8 assembly Hex-Quad-Hex assembly does not converge because it is not completely topologically interlocking in both dimensions. Here you can see that the 3x3 assembly when subjected to a normal displacement outside the plane of the assembly, fails to transfer the load across the adjacent shape in the front. It is because the nature of the contacting surface is planar and the front shape is completely below the displaced shape. Note that the boundary surfaces are always fixed.

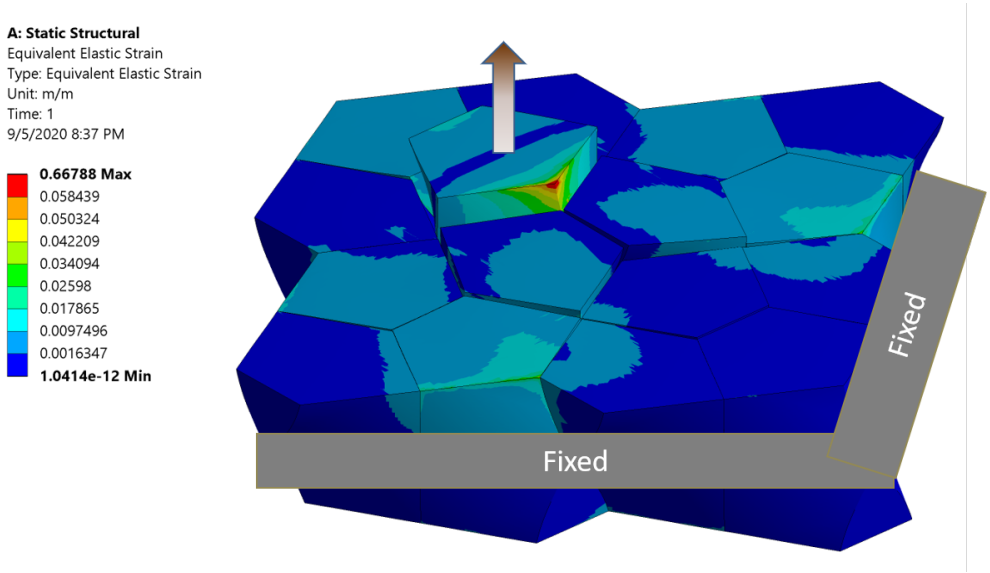

Figure 3.18: A pentagonal assembly is subjected to a lateral displacement out of the plane of assembly. The figure shows the contour plot of the strain across the assembly. The boundary surfaces are fixed. We can see the the shape distributes the load in both directions leading to a stable interlocking.

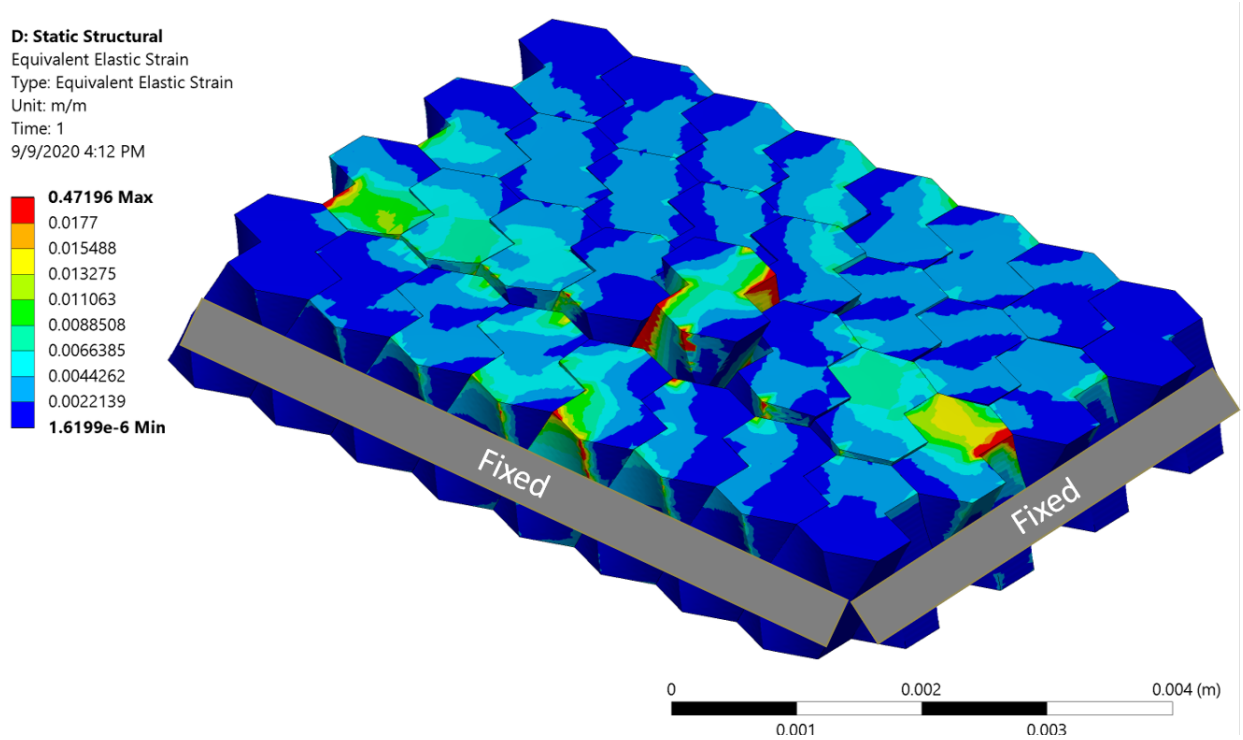

Figure 3.19: This the FEA result of an 8x8 assembly of Hex-Quad-Hex delaunay lofts. The shapes, however are not individual, but grouped pair wise. The simulation converges and we see that the load is distributed throughout the assembly in both directions. Note that the boundary surface are always fixed.

repeatable shapes. Here, our approach offered a unique advantage. The first condition is naturally satisfied by the strategy to use Voronoi partitioning (since any such partitioning is guaranteed to void-free for any given dimension). Therefore, the watertight condition is satisfied regardless of how the Voronoi sites are distributed on each of the extremal surfaces (as long as we can establish a on-to-one correspondences between the sites on each surface). We then addressed the second condition of repeatability through our method of construction and design based on wallpaper symmetries. Combining these two components resulted in a simple yet powerful methodology.

Ours is probably the first to apply geometric reasoning to describe a bio-physical phenomenon in order to apply it to 2.5D tiling design in a systematic manner. Our approach provides a possible explanation for the occurrence of scutoids in skin cells [2] and demonstrates the construction of many other shapes similar to scutoids.

Having said this, we would also like to point out that it is still to be completely tested that the method that we propose here for constructing Delaunay Lofts can indeed also be used to model the original scutoids. The key gap that needs to be addressed for this is to compare the actual geometry (and not the idealized model shown in Figure 3.2) that is experimentally obtained with one constructed using our approach with the same initial conditions as the bio-physical case.

3.8.2 Geometric Design Space

The design space of shapes that can be composed using our approach is unusually rich. This is due to three facts. First, the construction algorithm does not assume any specific shape of the control curves — as long as they intersect each slicing plane at a unique point thus maintaining the number of sites per slice. This alone provides many possibilities in terms of obtaining seemingly complex geometries. Second, the 17 wallpaper symmetries result in several possibilities in terms of the tiling configurations that may be possible with our approach. Finally, the distance functions utilized in all our examples are only L^2-norms. Generalizing to L^p-norms will lead to even more unusual shapes that we have currently demonstrated. Having said this, we have currently exposed only a limited set of repeatable tiles as examples in the paper. We are currently developing a more systematic geometric kernel and interactive software to explore the complete design space of

Delaunay Lofts.

3.9 Limitations of the 2.5D algorithm

Although the input for creating Delaunay Lofts are line segments, the shapes are merely computed by 2D Voronoi partitioning with points in every layer. There are some shortcomings of this approach that restricts us to explore Voronoi decomposition with free-form Voronoi sites. The primary disadvantage of this approach is that the number of Voronoi sites in every layer needs to be same. In other words, all the line segments should start from the bottom plane and end at the top plane. Line segments that are not touching the top and bottom plane will be considered as invalid inputs to the algorithm. Moreover, the line segments that define the Voronoi partitioning cannot be intersecting. That is, the assumptions posed on the line segments that we give as input to the Voronoi algorithm does not allow for tree-like or branch-like voronoi sites. In the next chapter, we will see how we can overcome this limitation using 3D Voronoi based algorithm. This freedom allows for designing shapes that are more topologically interlocking.

3.10 Conclusion and Future Work

We presented an approach to construct and eventually design a new class of tilings in 3D space. We have developed an algorithm that takes as input two planes containing Voronoi tessellations based on some distribution of points and interpolates the tilings between these given planes. The volumetric structures obtained through this interpolation result in the occurrence of Delaunay Lofts. There are several variations of how this interpolation can lead to a variety of such Lofts.

The future work is to investigate the power of shapes that are created by our bio-inspired design approach in terms of withstanding stress, torsion or fatigue. If these approaches can create powerful shapes in terms of withstanding stress , torsion and fatigue, this approach could be arguably applied to come up with completely new designs and structures that could have greater strength. An advantage of our approach is that it can easily be used in combinatorial optimization. Therefore, this approach could take the industry to the next level of material optimization and unveil endless possibilities of geometric designs with Delaunay Lofts.

	Scutoids	Delaunay Lofts	Means
Void-free and watertight	✓	✓	Voronoi Partitioning
Replicas can pack with each other	✗	✓	Wallpaper Symmetry
Control over topology shift	✗	✓	Quad Layer
Topological Interlocking	⚠	⚠	Better Control Curves

Figure 3.20: Table summarizing the properties of Delaunay Lofts

In the context of topological interlocking, Delaunay Lofts fails to show a reliable interlocking capability. While operations like 'grouping' shows some potential for for better interlocking, the simulations carried out for shapes generated individually does not guarantee interlocking. In the next chapter we propose an algorithm using 3D Voronoi decomposition that overcomes the limitations of layer-by-layer algorithm proposed in this Delaunay lofts that allows for free-form exploration of shapes with higher dimensional voronoi sites. We use this freedom to create Voronoi sites based on the canonical topologically interlocking Abeille vault to design space-filling shapes that are guarenteed to be topologically interlocking.

4. GENERALIZED ABEILLE TILES*

In the previous chapter, we saw how we can use a number of line segments between two parallel plane as controlling entities to create an shapes that are space-filling using 2D Voronoi partitioning layer-by-layer. Specifically, we showed the vast design space of repeating shapes can be generated using Wallpaper symmetry groups to points in the top and bottom planes. Finally, we highlighted the limitations of 2.5D construction algorithm to create free-form shapes and also the lack of significant topological interlocking for the shapes generated.

In this work, we extend the exploration beyond simply considering line segments as control curves by allowing allow control curves to be have branches and surfaces. To achieve this, we use the concept of 3D Voronoi decomposition with higher dimensional Voronoi sites. We then tune the control curves based on the symmetry of fabric weaves. In this chapter we will first see the 3D Voronoi algorithm that we use to construct the shapes from the control curves. Then, we will see how to design control curves inspiring from the current topologically interlocking shapes leveraging on our algorithm.

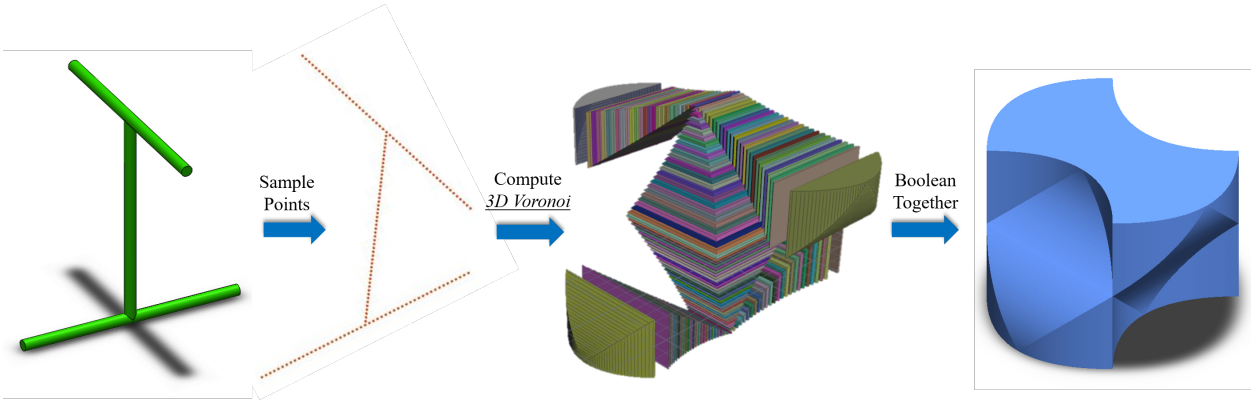

Figure 4.1: 3D Voronoi boolean Algorithm

*Part of the data reported in this chapter is reprinted with permission from "Generalized Abeille Tiles: Topologically Interlocked Space-Filling Shapes Generated Based on Fabric Symmetries" by Akleman, Ergun, et al, 2020. *Computers & Graphics*, 89, Page range 156-166 including figures 4.2, 4.3, 4.4, 4.6 and 4.7

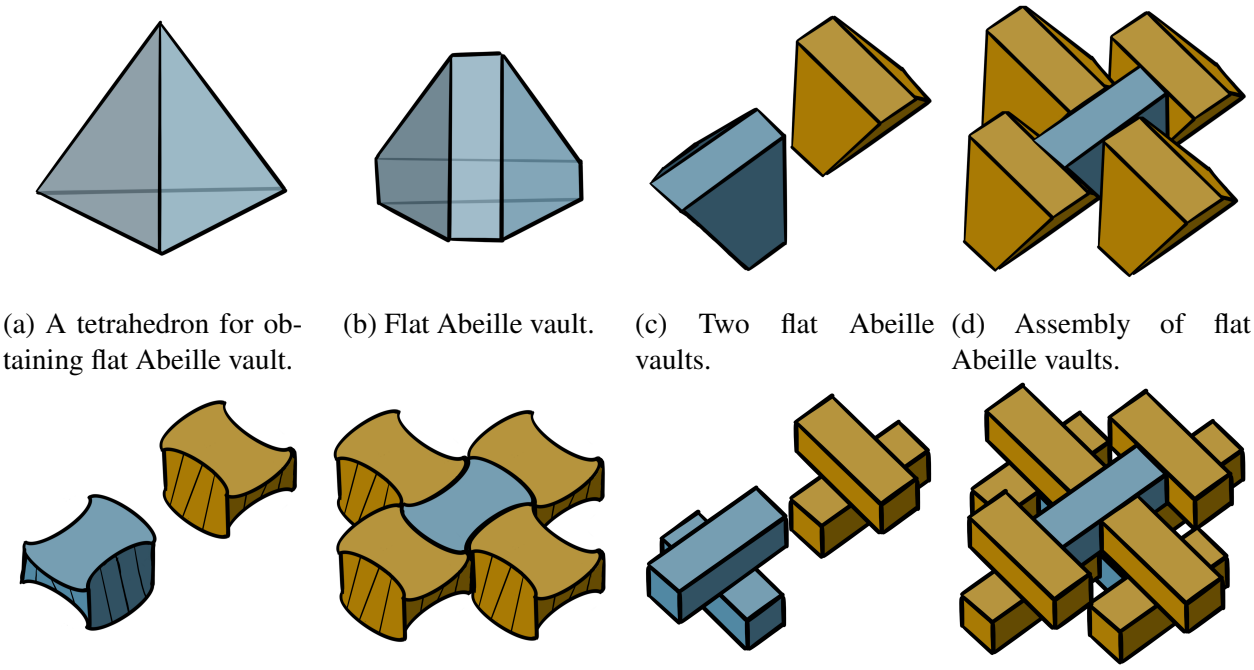

(a) A tetrahedron for obtaining flat Abeille vault.

(b) Flat Abeille vault.

(c) Two flat Abeille vaults.

(d) Assembly of flat Abeille vaults.

(e) Two Abeille vaults with circular edges.

(f) Space filling assembly of 4.2e.

(g) Two Abeille type discrete elements.

(h) Assembly of 4.2g.

Figure 4.2: (Hand-Drawn Illustrations) Abeille tiles are mirror symmetric structures obtained by placing two identical shapes placed on top of each other with a relative rotation of 90^0. Each elemental shape is generated by truncating two opposite edges of a tetrahedron. Notice that yellow and blue tiles have identical shapes. We added 4.2h to visually demonstrate that these assemblies can be achieved using symmetry operations of plain woven fabrics as shown in 4.2g.

4.1 3D Boolean Voronoi Algorithm

Using 3D Voronoi decomposition is a simple and intuitive way to extend our Delaunay Lofts algorithm to higher dimensional Voronoi sites. In Delaunay Lofts algorithm, we essentially combined all 2D convex polygons obtained after performing Voronoi decomposition in every layer. 3D Voronoi decomposition with points as Voronoi sites would give us convex polyhedras. Now, the algorithm basically is to take the union of convex polyhedra resulted from 3D Voronoi decomposition of 3D points. We also need to consider only a fundamental domain.

Taking union of all Voronoi regions belonging to the same guide shape (Voronoi site) to obtain desired space filling tile can be implemented as a set of face removal operations. Specifically, the shared faces of two consecutive convex polyhedra coming from two consecutive sample points

on the curve are deleted. Note that these faces will always have the same vertex positions with opposing order. If underlying mesh data structure provides consistent information, this operation is guaranteed to provide a 2-manifold mesh. Even if the underlying data structure does not provide consistent information, the operation creates a disconnected set of polygons that can still be fabricated through additive manufacturing.

4.2 Redesigning Control Curves

We designed several specific types of tiles by choosing Voronoi sites from basic property of Abeille tiles: two mirrored and 90^0 rotated shapes that are placed top of each other as shown in Figure 4.2g. These Voronoi sites can simply be a shape that connects two perpendicular lines as shown in Figure 4.3.

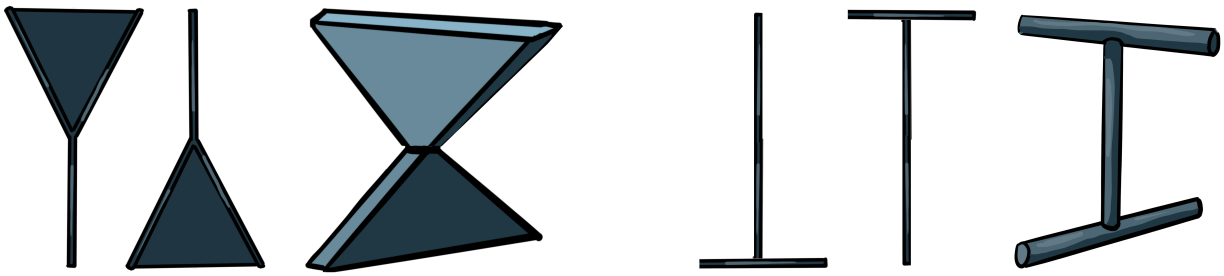

(a) Two mirrored and 90^0 rotated triangles.

(b) Two mirrored and 90^0 rotated T shapes.

Figure 4.3: (Hand-Drawn Illustrations) Front, side and 3D perspective view of the basic Voronoi sites we have initially used to obtain space filling Abeille tiles.

The Voronoi site shown in Figure 4.3a consists of two triangles that can be converted into a GAT by using layer-by-layer 2D Voronoi decomposition. When we use 3D Voronoi decomposition, it is possible to simplify Voronoi sites into a T-shaped configuration as shown in Figure 4.3b. Section 4.1 discuss 3D Voronoi decomposition to create the GATs. These basic structures are assembled using symmetry operations of two-way two-fold woven structures.

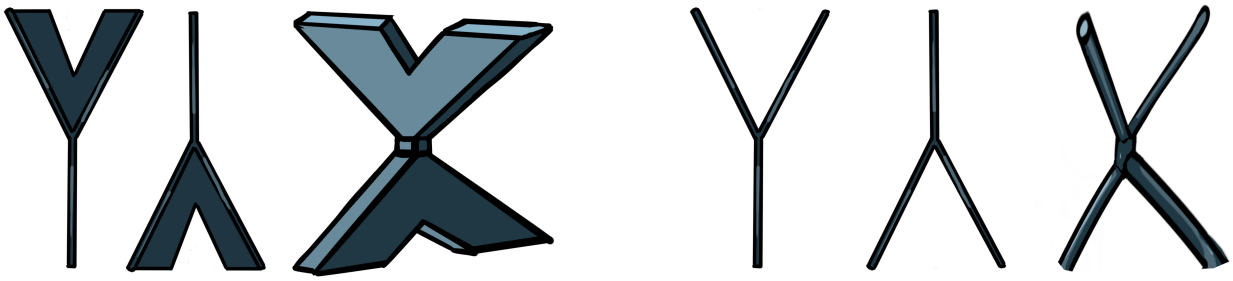

(a) Two mirrored and 90^0 rotated concave hexagons.

(b) Two mirrored and 90^0 rotated V shapes.

Figure 4.4: (Hand-Drawn Illustrations) Front, side and 3D perspective view of V shaped Voronoi sites we have used.

4.3 Structural Evaluation

The mechanics and geometry of Abeille-type structures are closely connected as shown earlier by Brocato et al. [49, 41, 45]. These mechanical investigations are primarily focused on the interaction between the faces in contact between two adjacent pieces — what Brocato et al. refer to as Abeille-bond. Therefore, the overarching topology of the structure/assembly composed of the Abeille-shaped "*bricks*" has a major effect on the mechanical behavior of the structure. Our aim was to observe how different weave symmetries induce different mechanical behavior compared to the flat Abeille vault. For this, we conducted several simulations of GAT assemblies using finite element analysis (FEA) and compared them with Abeille's original flat vault as well as a solid object as our benchmark.

4.3.1 Evaluation Rationale

Consider a solid continuous rectangular block of some finite thickness fixed to an inertial frame on the boundaries. Now, let us suppose that the center of this block is displaced by some load along the thickness of the block. In the context of topological interlocking, the stress distribution induced by such a displacement on this block represents our absolute benchmark. Therefore, in our evaluation, we seek to investigate the inter-locking properties of GAT assemblies by comparing the magnitude and concentration of stresses induced by a displacement of one tiles (say the central tile

without the loss of generality). We further note that high stress regions will occur at the interacting surfaces between two neighboring tiles. With this in view, we make three main observations: (1) higher magnitude of interface stress will imply better inter-locking; (2) the regularity of distribution and concentration of stress will imply better stability against perturbations in loading conditions.

Block Equivalent: In order to compare with our benchmark scenario, our first step was to conduct FEA simulations on a solid block of dimensions identical to the assemblies (box equivalent). The mechanical properties of this box equivalent would serve as a reference for us to compare the degree of tightness of inter-connectivity in between the unit GATs.

Flat Abeille vault: We further wanted to evaluate Abeille's original vault design. Abeille's original flat tiles are parametric structures which can be arranged together to form an assembly (Figure 4.2d). This assembly, though not space filling, can be held together simply by fixing the tiles in the perimeter. Khandelwal et al. [88] showed that the force–displacement response for topologically interlocked structures, specifically based on Abeille's flat vaults, exhibited an ideal softening response even though the individual blocks (tiles) were made out of brittle material. We study the mechanical response of these tiles separately and also compare it with the results we obtain for GATs.

Generalized Abeille Tiling: The shape of a unit GAT depends on two key factors. The first is the construction methodology (layer-wise 2D or 3D Voronoi decomposition). The second is the shape of the Voronoi sites. While the construction methodology results in minor differences between the shapes (in terms of continuity and smoothness of the contact surfaces), it is the configuration of the Voronoi sites that fundamentally affects the shape of each unit tile and consequently the interactions between those unit tiles in a given assembly of tiles. Furthermore, notice that the configuration of the Voronoi sites is based on the symmetries of the fabric weaving patterns. Therefore, in order to explore the relationship between the weave symmetries and the corresponding GATs, we considered two commonly known plain and twill weaves and analyzed their response to basic mechanical loading conditions. We specifically investigated the following cases:

1. **PA2D**: Plain-Abeille tiles generated with T-shaped Voronoi sites.

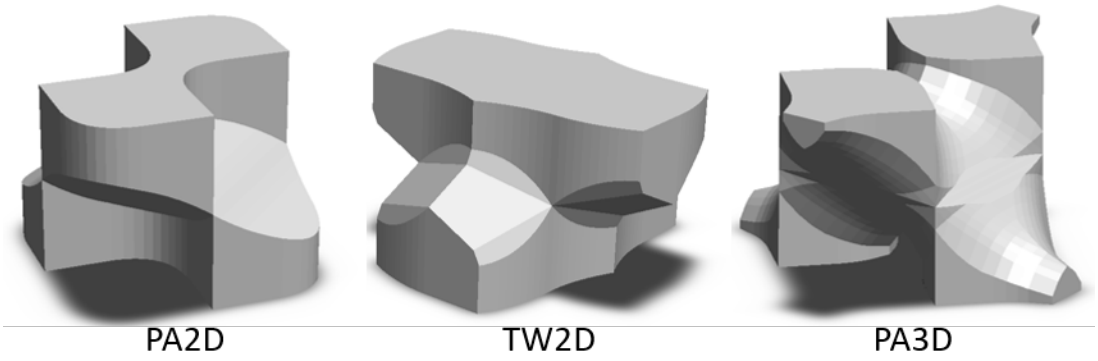

Figure 4.5: Resulting shapes obtained for three specific cases. There are two variables to choose from. One, the choice of weave pattern. Two, the choice of control curve — V-shape or T-shape.

2. **TW2D**: Twill-Abeille tiles generated with T-shaped Voronoi sites.

3. **PA3D**: Plain-Abeille tiles generated using with V-shaped Voronoi sites.

4.3.2 Evaluation Methodology

We assembled a 7×7 grid of the three GAT cases without any gaps between the parts. The contacts between the tiles are assumed to have zero friction. A displacement of 2mm was assumed to act vertically upwards out of the plane of the assembly. The border tiles in the assemblies were assigned as fixed supports. All possible contact regions between were made friction-less. This ensures that the stress induced in the assembly is solely due to the geometry of the tile itself. Mesh quality was set to default (0.5). The von-mises stress [89] and the total deformation color plots are then computed for each case (Figure 4.6). We conducted a static structural analysis for all simulations using the ANSYS Workbench 2019 R1.

Assumptions: The volume of each of the unit shapes is assumed (and modeled) to be equal. This, allows to make a fair comparison of the behaviour of these shapes when subjected to loading. Appropriate end faces were assumed as fixed support for every simulations and all the forces and moments were applied on the faces directly. All the simulations are done by assuming appropriate faces of central tile displaced by a constant distance of 2mm. All materials were assumed to be Polylactic acid (PLA) (density $= 1250\ kg/m^3$, Young's modulus $E = 3.45 \times 10^3 MPa$, Poisson's

Ratio $\nu = 0.39$).

4.3.3 Results and Observations

4.3.3.1 GATs vs Box equivalent

Since the block essentially represents a continuous connected version of the assembly it would offer the highest resistance to external disturbances. This can be be seen from the maximum value of average stress (20.35 Pa). We find that the average stress induced in the 3 cases **PA2D**, **TW2D**, and **PA3D** is of the same order of the Block equivalent.

The block has three regions of displacement: (1) constant region at the center, (2) a linearly decreasing region from the center to periphery, and (3) fixed periphery (Figure 4.6). Interestingly, the **TW2D** pattern exhibits similar displacement profile. On the other hand, the **PA2D** and **PA3D** cases exhibit a decreasing continuity in the displacement profile. **PA3D** specifically shows a highly local displacement profile suggesting a higher interlocking ability again owing to the V-shaped Voronoi site. Finally, we note that the average displacement for the GAT assemblies are all lesser (albeit marginally) than the solid block. This, again, indicates good inter-locking ability.

4.3.3.2 GATs vs Flat Abeille Vault

The values of stresses found in the flat Abeille vault, however, are orders of magnitude lesser than any of the GATs tested (Table 4.1). This clearly shows that the Abeille tiling may not offer high resistance to external disturbances compared to GATs. The implication is that GATs are tightly topologically interlocked when compared to flat Abeille vaults. The second crucial observation we made was that lack of symmetry in stress distributions for Abeille's flat vaults despite the fact that the assembly follows plain woven weave symmetry aking to some of our own assemblies. To investigate this further, we performed additional tests wherein we displaced different combinations of faces on the central element of the tiling. The resulting stress distributions still do not exhibit any observable symmetry or even consistency with respect to the other loading variations. This strongly indicates the lack of structural stability meaning that small perturbations in load can lead to large variations in how stresses are distributed to neighboring elements. We believe that the

	Block	**PA2D**	**TW2D**	**PA3D**	Abeille
Stress (MPa)					
Min.	3.11e-11	1.15e-6	7.28e-1	9.45e-10	1.81e-14
Avg.	20.35	7.78	9.97	7.87	2.75e-9
Max.	94.18	232.2	404.82	153.02	2.86e-7
Displacement (m)					
Min.	0.00	0.00	0.00	0.00	0.00
Avg.	4.69e-4	3.46e-4	3.71e-4	3.15e-4	3.51e-4
Max.	2e-3	2e-3	2e-3	2e-3	2e-3

Table 4.1: Minimum, maximum and average stresses and displacements for tile assemblies when the center tile is subjected to a displacement of 2mm.

primary reason for this is the planar interface between two Abeille elements as opposed to curved convex-concave interfaces in GATs. This geometric property of GATs allows for a smoother propagation of contact stresses between neighboring elements resulting in a topologically consistent stress distribution.

4.3.3.3 Stress distribution patterns in GATs

Each of the three GAT cases exhibit distinct stress distribution patterns. Our goal is to compare these with the solid cuboidal block that exhibits a radially smooth variation of stress with concentration near the boundary which is fixed. In case of **PA2D**, we observe that the stress distribution is separated in two mutually perpendicular directions corresponding to the two axes of the bi-axial plain weaves. What is interesting is that the stresses on the top and bottom layers alternates between tiles aligned along the same direction, This is because a majority of stress transfer between two orthogonal tiles primarily takes place in the neck region of the tiles. For **TW2D**, we notice that the stress on the top and bottom layers is more uniformly distributed. However, this too alternates across orthogonal tiles. The stress distribution for **PA3D** is the most sparse distribution shaped as two rings induced on either side of the V-shape. We also observe an outer octagonal ring. This is likely due to the inter-tile interactions between the shapes induced by the V-shaped Voronoi sites. Unlike GATs, the flat Abeille vault does not have any distribution pattern or symmetry as previously noted.

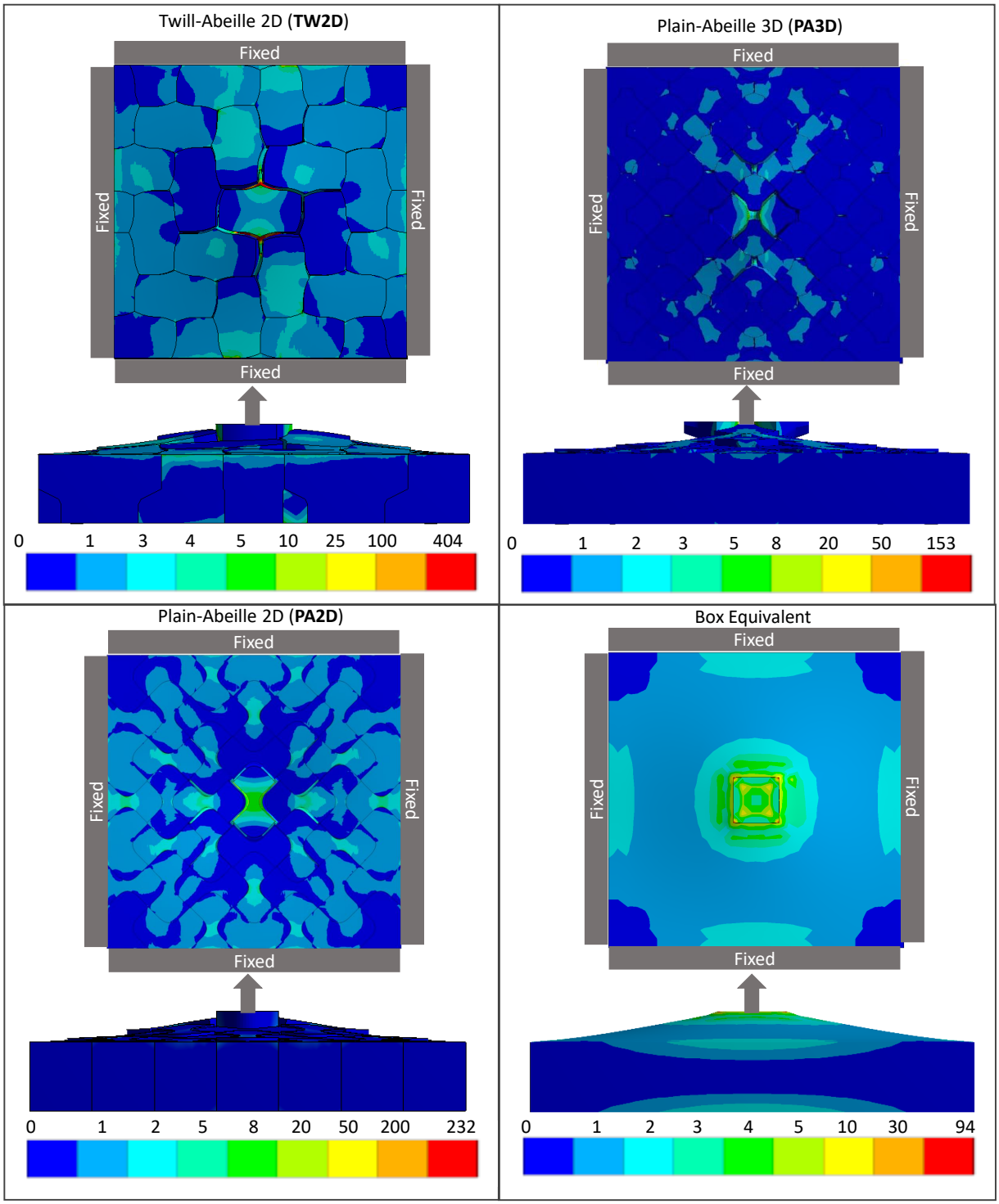

Figure 4.6: (Simulation) This shows the stress distribution on a 7x7 assembly of various generated shapes. This can all be compared with the single block equivalent of these assemblies. The top and side view are shown such that the forced displacement can be seen. A displacement of 2mm was forced on the center tile. All stress values are in MPa.

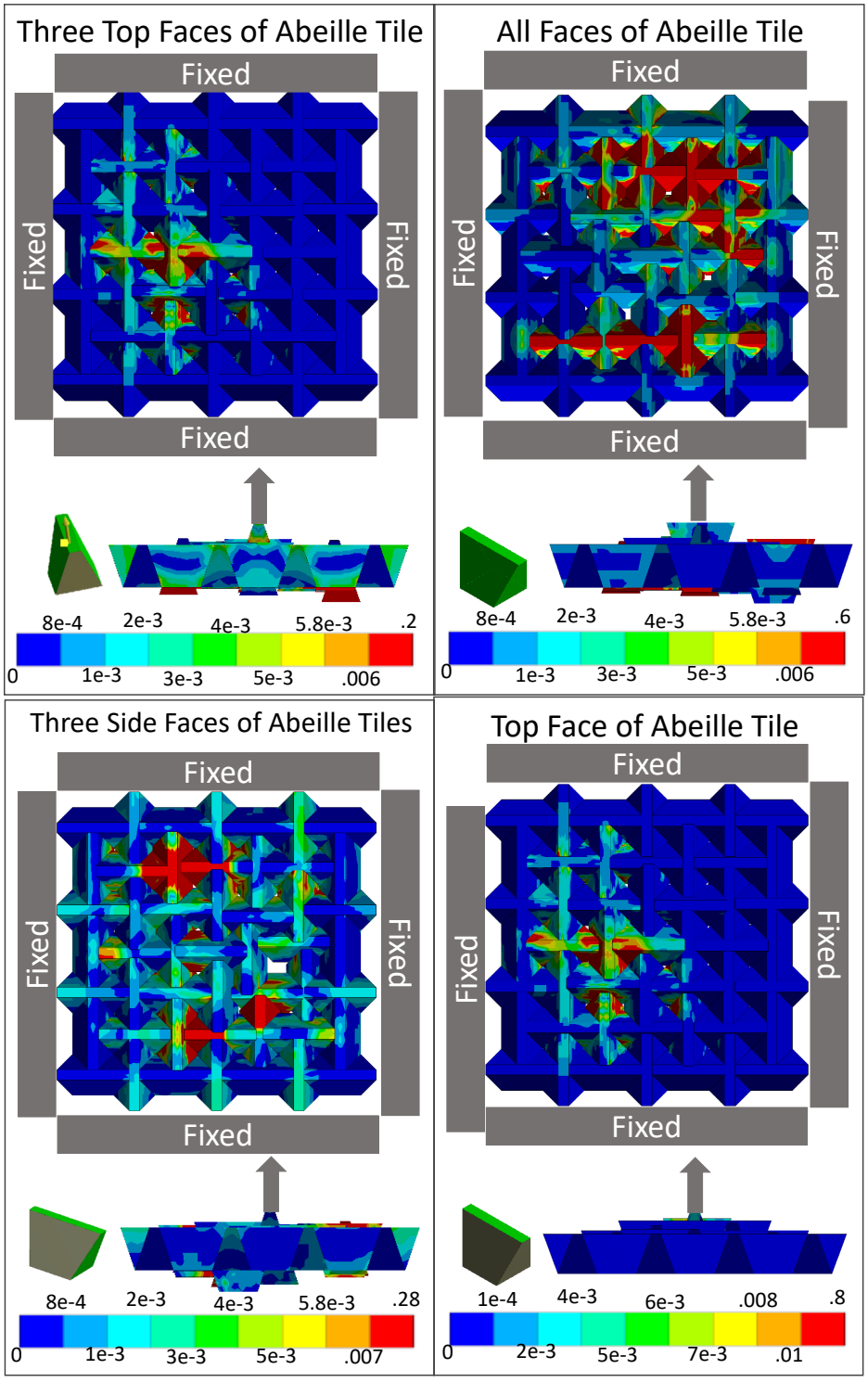

Figure 4.7: (Simulation) This shows the stress distribution on a 7x7 assembly of Abeille tiles with different amounts of faces with forced displacement. In the first case the top face and the two larger side faces were forced with a displacement of 2mm. The third case shows when the top face and the two smaller side faces have a forced displacement. All stress values are in Pa. This means there is very little force needed to get a displacement of 2mm.

	Delaunay Lofts	GATs	Means
Void-free and watertight	✓	✓	Voronoi Partitioning
Replicas can pack with each other	✓	✓	Weave Symmetry
Free-form Control Curves	✗	✓	3D Partitioning
Topological Interlocking	⚠	✓	Inspiration from Abeille

Figure 4.8: Comparison of Generalized Abeille Tiles with Delaunay Lofts

4.3.3.4 Comparison across GATs

We observe a dissimilar behavior between **PA2D** and **PA3D** assemblies in terms of the maximum stresses (232.2 MPa and 153.02 MPa respectively). However, the average stresses are similar (7.78 MPa and 7.87 MPa) for these two cases when compared to **TW2D** (9.97 MPa). The most noticable observation is that the **TW2D** tiles experience the highest extremal stresses (7.28e-1 MPa and 404.82 MPa) in comparison to the other two cases. This is likely because of the high curvature neck regions in the **TW2D** tiles.

4.4 Summary of Generalized Abeille Tiles

The primary limitation of the shapes that we obtained from Delaunay Lofts is that it failed to show considerable topological interlocking. In this chapter, we showed how we can overcome the limitation by leveraging a visual correspondence between the Abeille vault and the symmetry of fabric weaves. Then, inspired from the symmetry of fabric weaves, we developed control curves that generate shapes that are ensured to be topologically interlocking. We used a Boolean of 3D Voronoi partitions to obtain the corresponding Generalized Abeille Tile. We validated the interlocking capabilities of the GATs by doing a structural evaluation using FEA. We also showed that Generalized Abeille Tiles have a distinct stress distribution pattern compared to an inconsistent stress distribution with respect to loading variations in Abeille vault. The magnitude higher

stress magnitude induced in the assembly were also ordered of magnitude higher in GATs compared to Abeille vault suggesting the better interlocking capabilities of GATs. We believe that the emergence of the interesting stress patterns has a strong relation with the choice of the controlling Voronoi sites.

4.5 Comparision with Delaunay Lofts

To obtain these shapes, the Voronoi sites typically need to be made of branches and surfaces as opposed to line segments in Delaunay Lofts. This is made possible using 3D Voronoi partitioning algorithm and 'grouping' together the Polyhedrons (or convex volumes) that belong to a control curve. Note that this is similar to the grouping experiment that we did in section 3.7.4 except that we did not have rationale for choosing the entities that we are going to group together in section 3.7.4. The fundamental difference that makes this approach better is that we group the entities based on the control curve that every belongs to and not intuitively. Figure 4.8 shows the comparison of GATs with Delaunay Lofts across different factors.

5. CONCLUSIONS

This chapter is organized as follows. In section 5.1, we summarize the contributions of this research. Then we highlight the limitations (section 5.2), future directions (section 5.3) and broad implication (section 5.4) of this work and finally end with concluding remarks. (section 5.5)

5.1 Summary of Contributions

5.1.1 Methodology for Creating Void-Free Shapes

We are the first to take the notion of Scutoids that occurs in a particular situation in nature and converted it into an elegant design methodology to create shapes that we didn't even know existed before. We present a simple and intuitive approach for designing space filling tiles in 3D space. 'Scutoid' shapes were recently reported to occur in epithelial cells due to topological changes between the extremal (apical and basal) surfaces of epithelia. Drawing from this discovery, we develop the theoretical and computational foundations leading to a generalized procedure for generating Delaunay Lofts — a new class of scutoid-like shapes. Given two extremal surfaces, both with Delaunay diagrams, Delaunay Lofts are shapes that result from Voronoi tessellation of all intermediate surfaces along the curves joining the vertices of Delaunay diagrams that defines the extremal tessellations. We show that two algorithms for computing the Voronoi partitioning with higher dimensional sites (lines instead of points) in 3D space. Thus, we show that the shapes thus obtained by our methods are guaranteed to be watertight or void-free.

5.1.2 Methodology for Creating Repeating Shapes

Secondly, we proposed two concepts for create repeatable tiles — wallpaper symmetry groups and the symmetry of fabric weaves.

5.1.2.1 Wallpaper symmetry groups

We apply the symmetry of Wallpaper groups on points to obtain a pattern of points in 2D. Using Wallpaper symmetry groups allowed us to exhaustively characterize all possible 2D patterns. We

modify the position of points to obtain two sets of points in in two layers. The line segments joining the corresponding points between the two plane will serve as the input for obtaining the voronoi decomposition. We show that the resulting shapes repeat and fill the 3D space individually (regular tiles) or sometimes combined with adjacent shapes in the decomposition (semi-regular tiles).

5.1.2.2 Fabric weave symmetry

Drawing a visual analogy between symmetries of plain woven fabrics and assembly of truncated tetrahedra (and their variants) that are used in topological interlocking, we leverage this correspondence to develop a methodology based on symmetry of fabric weave to design control curves whose Voronoi decomposition are **ensured to create topologically interlocking shapes**.

5.1.3 Better Topologically Interlocking shapes

Thirdly, we ensured that our method does create stronger topologically interlocking shapes by performing a comparative structural evaluation of three specific tiles generated by plain and twill woven fabric symmetries. The finite element analyses (FEA) of the unit tiles and their assemblies under different loading conditions reveal that weaving allows distribution of planar and normal loads across tiles through the contact surfaces, generated with our methodology. We describe the qualitative relationship between the symmetries induced by the weave patterns to the stress distribution in the tiled assemblies. Through FEA, we also show that flat Abeille does not offer high resistance to external disturbances.

5.2 Limitations

5.2.1 Generalized Abeille Tiles

There are several limitations of our design methodology for generalzied Abeille tiles. First, in the current work, we focus on only symmetries of 2-way 2-fold fabrics to simplify our explorations. Even simply considering the symmetries of 3-way 2-fold fabrics can significantly extend the design space [90]. Second, although the resulting tiles will still be space-filling (owing to Voronoi partitioning), the connections in z-direction are not really interesting: they are flat. For true 3D space filling tiles, the symmetries must go beyond 2.5D symmetries that are extended from 2D

wall paper symmetries such as symmetries of 2-fold fabrics. Third, we considered decomposition of only 2.5D flat shell structures. In order to construct curved shell structures, one may need more than one unique shape for a tile. Generating GATs for curved boundaries needs to be explored in detail. Finally, and most importantly, our work currently allows only for the *forward design* of space-filling tiles. However, what would be more interesting for structural applications is to be able to specify desired physical characteristics to automatically configure the weave-symmetries and Voronoi sites to create GATs. While we initiated structural characterization in this work, we believe that a much deeper analysis of geometry-to-structure relationship needs to be developed for *inverse design* of GATs.

5.2.2 Geometric Modeling Methodology

The smoothness of resulting shapes in both of our algorithms are sensitive to disretization of control curves. In Delaunay Lofts, we were essentially discretizing the region in between the two parallel planes to obtain a number of layer that would serve as a reference for finding and stitching our Voronoi polygons. In the algorithm presented in Generalized Abeille Tiles, the approximation of the shape is directly dependent on the sampling along the control curve. Note that increasing the sampling rate always comes at the cost of increasing time complexity given that we are using 3D Voronoi for computation.

5.2.3 Physical Evaluation

In physical evaluations of the generalized Abeille tiles we have only considered 3 specific shapes and compared the results with a monolithic block and assemblies made of Abeille vault. While this helps us highlight the potential of our method to create better interlocking shapes, an even more rigorous analysis is necessary to characterize the mechanical behavior of entire design space. We believe that there are interesting properties that can be discovered based on the stress patterns and the corresponding mechanical properties. Also, the individual blocks when considered as rigid bodies would help in understanding the nature of force transfer in a simpler and faster way. Effect of properties like tolerances and friction in the surface of the block also need to

be included in the simulation setting to make the simulation more real-world and practical. A simple alternative to simulation would be to do the physical testing of assemblies of interlocking shapes. The shortcomings of FEA can easily be overcome by performing physical testing since it automatically incurs the real world constraints.

Also, in Section 3.7 and 4.3 we made predictions on degree of interlocking of different types of repeating shapes. Currently, our strategy for characterizing the degree of interlocking is based on the magnitude of maximum, average and minimum stress and strain in the assembly. In the future we need a more robust methodology to characterize the degree of topological interlocking more precisely. Finally, our comparison with other topologically interlocking tiles in this work has been limited to just Abeille's fault vault, however, this comparison needs to be extended other assemblies like Osteomorphic blocks in the future.

5.3 Future Directions

5.3.1 In-fills for 3D Printing

A recent research [91], proposed a geometric modeling methodology for generating a new class of infills for additive manufacturing. They showed that an infill pattern can simply be instantiated using a 2D point distribution according to a chosen wallpaper symmetry and performing 2D Voronoi partitioning. In fact, some of the common extruded infills (hexagonal, square, and diamond) are essentially special cases of wallpaper-infills generated by specific point arrangements in the plane. They also conducted a detailed experimental evaluation of the of these four cases to study their mechanical behavior under tensile loading and showed that the designed infills provide a wide range of elongation that depends on the degree-of-freedom associated with the space-filling polygon generated by a given wallpaper symmetry. We believe that there is a rich design space of new in-fills that we can obtain by changing the orientation, point distribution and varying angles of the controlling line segments by using 2.5D Voronoi algorithm described in Chapter 3.

5.3.2 Generalization with Knots and Links

2-fold fabric structures are much richer than just 2-way genus-1 fabrics. Their real power can be best understood with extended graph rotation systems (EGRS) that was introduced in early 2010's [92, 93]. EGRS allows us to use orientable 2-manifold meshes as guide shapes to represent knots and links. The guide shapes help us to classify the fabrics. For instance, the guide shapes for 2-fold 2-way fabrics are regular grids embedded on genus-1 surfaces. For 2-fold 3-way fabrics, we need regular hexagonal or regular triangular grid embedded on genus-1 surfaces [92]. This is useful since some of the Leonardo grid designs are based on also 3-way woven patterns [94]. Using regular maps [95, 96], it is also possible to obtain hyperbolic tiling. Using the regular maps that correspond to hyperbolic tiles as guide shapes, 2-fold k-way genus-n fabrics can be obtained. From these fabrics, one can also obtain space filling shapes. For practical applications, there is a need for a significant amount theoretical work.

5.3.3 Metamaterials designs

An interesting application using the space decomposition algorithm is the designing of Metamaterials designs — materials that have properties that are not found in naturallu occurring materials. Cell, frame and lattice-based structures are extensively used to design materials with controllable mechanical properties. Our algorithm of space decomposition provides divides a given domain into regions. The boundary shared by these regions are defined by the position of the Voronoi sites that we provide as input. In 3D, these boundaries are typically surfaces that are formed as a result of equidistant relation between the Voronoi sites. We created algorithm to generate material by thickening these boundary surfaces. The algorithm, builds on the layer-by-layer 2.5D Voronoi algorithm described in Section 3.3. For every convex Voronoi polygon in every layer, we offset the polygon inside that eventually creates a shell of the surface. Finally, we bound the top and bottom shell regions to obtain a water-tight manifold mesh (see Figure 5.1)

The advantage of using the method of Voronoi decomposition to generate the material is that we have a direct control over Voronoi sites. This allows us to tune and spatially vary parameters

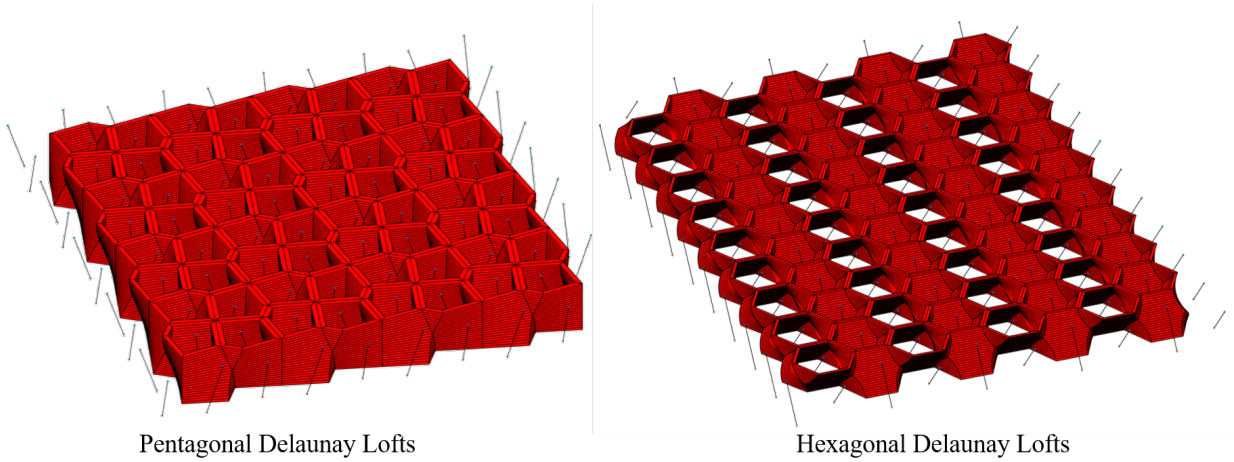

Figure 5.1: Pentagonal and Hexagonal metameterial generated using our algorithm. The line segments in the middle of every hole (in place of the shape) are the corresponding Voronoi sites.

of the line segments, to easily obtain materials with spacially varying properties. We created an example of with the hexagonal Delaunay lofts by varying the relative angle in every row of the loft assembly. In Figure 5.2 we show a linear interpolation of the line angle with the plane of the assembly. However, such parameters can also be varied based on any desired function to create functionally graded materials. The challenge however, is to explore and characterize the mechanical behavior of metamaterial of the pure lofts, so that we can interpolate between them.

5.4 Implications

5.4.1 Geometric Interlocking

In a similar work, we use the 3D Voronoi algorithm with the weave based control curves that followed the wefts and warps. These tiles show some potential for geometric interlocking. Certain configurations structures can even create loops that are self interlocking. The advantage of self-interlocking or geometrical interlocking of shapes is that there is no necessity for external or peripheral loads to support the interlocking of tiles together. For these cases, we at least one flexible piece to lock the pieces together [97]. In the future, an interesting problem is to identify the number and position of these flexible pieces that is required to assemble the shapes together. Also, these flexible elements can be places inside the assembly at selected patterns at our will to allow

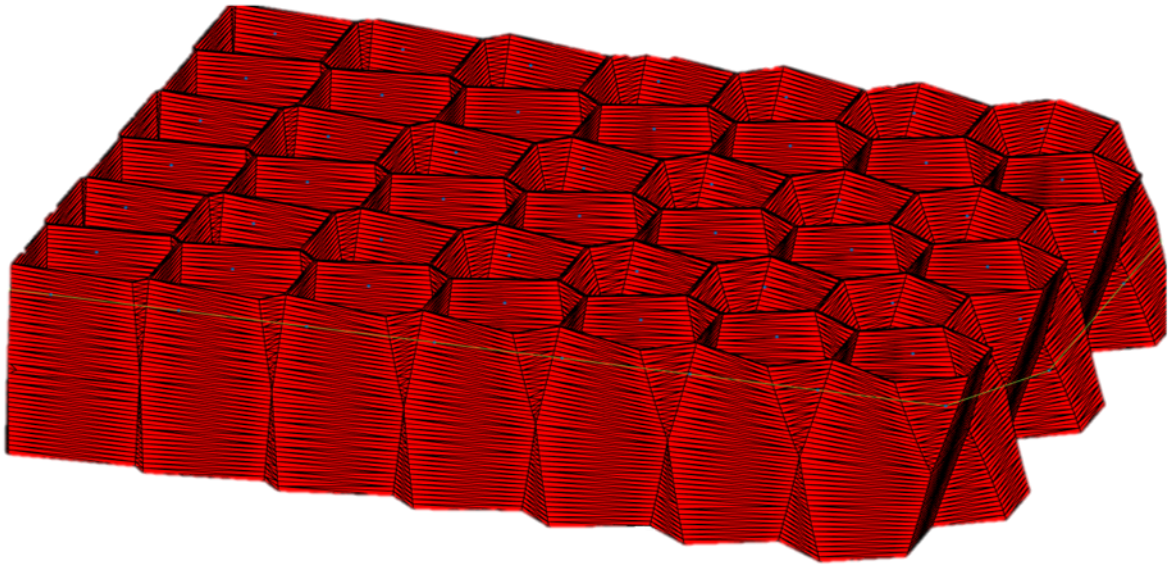

Figure 5.2: Material generated for hexagonal Delaunay lofts with varying angles across the rows. Note that the nature of the lofts changes from being close to a prism in the left to being the canonical hexagonal Delaunay lofts in the right.

for different mechanical properties of the assembly.

5.4.2 Chirality

Chirality is a key aspect of further investigation in this research. A recent work discovered how to produce handedness in auxetic unit cells that shear as they expand by changing the symmetries and alignments of repeating unit cells [98]. A similar work on designing geometrically interlocking shapes has explored the aspect of chirality in their shapes [97] more elaborately. Using the symmetry and alignment rules we can potentially expand our woven tiles to develop a new class of rigid and compliant structures [99, 100, 101]. Recent works on knot periodicity in reticular chemistry [102] and tri-axial weaves (also known as mad weaves) [103] are fundamental examples of how the geometry and physics of chirality are connected. Thus, identifying any fundamental multi-physical behavior of the assemblies shown in this work and beyond would allow us to construct assemblies with several practical applications such as mechanically augmented structures in mechanical, architectural, aerospace [104, 105], and materials [106] engineering. The main gap

that must first be filled, however, is a complete characterization of chirality of woven tiles including and beyond plain, twill, and satin varieties.

5.4.3 Reciprocity

Pugnale and Sassone [107] define the principle of reciprocity to be based on "*load-bearing elements which, supporting one another along their spans and never at the extremities, compose a spatial configuration with no clear structural hierarchy*". The idea of reciprocal frames dates back to ancient Indian, Chinese, and Japanese structures in the east as well as in the works of prominent designers of the west including Leonardo's. These have recently been studied and generalized in several works [108, 107, 6] from a structural standpoint. One of the most important observations here is that reciprocal frames are essentially characterized by the topological connectivity of the constitutive load-bearing beams — a trait also present in our own framework for generating GATs. One of the main outcomes of our structural analysis is the correspondence between fabric weave symmetries and the distribution of stresses on GAT assemblies. Specifically, our analyses indicate that the mechanical properties of a given fabric woven using a specific strand pattern can provide fundamental insights regarding GAT assemblies whose shape is generated using the same weave pattern. We believe that there is an even deeper connection across weave patterns, GATs, and reciprocal frames that may lead to a systematic framework for structural analyses of such systems.

5.4.4 Inverse Design

The unique stress patterns that emerge in our FEA results indicate that the weave parameters and the choice of line segment parameters (angle, length, etc.) affects the mechanical response directly. This raises the inverse question that if we are given with the mechanical characteristics whether we can find the parameters that define the geometry. Although our overarching goal throughout this effort was to see how geometry affects the mechanical behavior, our ultimate goal is to have a system where a designer come and give some kinematic or force constraints, and we generate the geometry automatically.

5.5 Concluding Remarks

An important problem with the current CAD software packages is representing and modigying complex geometries. The existing methods like B-rep and CSG forces the user to imagine how the geometry of the design should look explicitly, before starting to designing these shapes. This does not allow for intuitive, hand-drawn and free-form implicit control of the shapes. To this effect, our research provides a framework to translate the designer's intent (in the form of control curves or surfaces) to geometry of the resulting shape. This allows intuitive exploration of the shapes that are useful for early-stage design ideation.

Design optimization also requires that geometry remains topologically valid as parameters are perturbed while preserving the designer's intent [109]. So, simply by placing hard and soft constraints on the controlling entities that are representative of the shape, we explore a design space of shapes to optimize and best satisfy the user's objective. In this way, our techniques also hold a great potential to reduce the time and space complexity of optimization algorithms. To this end, we believe using our simpler shape representation techniques for a complex range of geometric surfaces will help developing more intuitive, creative and optimized designs.

REFERENCES

[1] A. F. Frézier, *La theorie et la pratique de la coupe des pierres et des bois, pour la construction des voutes et autres parties des bâtimens civils & militaires, ou Traité de stereotomie a l'usage de l'architecture*, vol. 2. Doulsseker, 1738.

[2] P. Gómez-Gálvez, P. Vicente-Munuera, A. Tagua, C. Forja, A. M. Castro, M. Letrán, A. Valencia-Expósito, C. Grima, M. Bermúdez-Gallardo, Ó. Serrano-Pérez-Higueras, *et al.*, "Scutoids are a geometrical solution to three-dimensional packing of epithelia," *Nature communications*, vol. 9, no. 1, pp. 1–14, 2018.

[3] E. Akleman, J. Chen, and B. Meric, "Web-based intuitive and effective design of symmetric tiles," *Proceedings of ACM Multimedia*, vol. 21, no. 4, pp. 100–108, 2000.

[4] M. Ashby and Y. J. Bréchet, "Designing hybrid materials," *Acta materialia*, vol. 51, no. 19, pp. 5801–5821, 2003.

[5] Y. Estrin, A. V. Dyskin, and E. Pasternak, "Topological interlocking as a material design concept," *Materials Science and Engineering: C*, vol. 31, no. 6, pp. 1189–1194, 2011.

[6] T. Siegmund, F. Barthelat, R. Cipra, E. Habtour, and J. Riddick, "Manufacture and mechanics of topologically interlocked material assemblies," *Applied Mechanics Reviews*, vol. 68, no. 4, 2016.

[7] S. Khandelwal, T. Siegmund, R. Cipra, and J. Bolton, "Adaptive mechanical properties of topologically interlocking material systems," *Smart Materials and Structures*, vol. 24, no. 4, p. 045037, 2015.

[8] A. L. Loeb, "Space-filling polyhedra," in *Space Structures*, pp. 127–132, Springer, 1991.

[9] B. Grünbaum and G. C. Shephard, "Tilings with congruent tiles," *Bulletin of the American Mathematical Society*, vol. 3, no. 3, pp. 951–973, 1980.

[10] E. Whiting, J. Ochsendorf, and F. Durand, "Procedural modeling of structurally-sound masonry buildings," *ACM Trans. Graph.*, vol. 28, pp. 112:1–112:9, Dec. 2009.

[11] M. Deuss, D. Panozzo, E. Whiting, Y. Liu, P. Block, O. Sorkine-Hornung, and M. Pauly, "Assembling self-supporting structures," *ACM Trans. Graph.*, vol. 33, pp. 214:1–214:10, Nov. 2014.

[12] E. Whiting, H. Shin, R. Wang, J. Ochsendorf, and F. Durand, "Structural optimization of 3d masonry buildings," *ACM Trans. Graph.*, vol. 31, pp. 159:1–159:11, Nov. 2012.

[13] H. V. Shin, C. F. Porst, E. Vouga, J. Ochsendorf, and F. Durand, "Reconciling elastic and equilibrium methods for static analysis," *ACM Trans. Graph.*, vol. 35, pp. 13:1–13:16, Feb. 2016.

[14] M. Kilian, D. Pellis, J. Wallner, and H. Pottmann, "Material-minimizing forms and structures," *ACM Trans. Graphics*, vol. 36, no. 6, p. article 173, 2017. Proc. SIGGRAPH Asia.

[15] G. Fallacara, "Toward a stereotomic design: Experimental constructions and didactic experiences," in *Proceedings of the Third International Congress on Construction History*, p. 553, 2009.

[16] A. Dyskin, Y. Estrin, A. Kanel-Belov, and E. Pasternak, "A new concept in design of materials and structures: Assemblies of interlocked tetrahedron-shaped elements," *Scripta Materialia*, vol. 44, no. 12, pp. 2689–2694, 2001.

[17] A. V. Dyskin, Y. Estrin, A. J. Kanel-Belov, and E. Pasternak, "Topological interlocking of platonic solids: A way to new materials and structures," *Philosophical magazine letters*, vol. 83, no. 3, pp. 197–203, 2003.

[18] A. Dyskin, Y. Estrin, A. Kanel-Belov, and E. Pasternak, "Interlocking properties of buckyballs," *Physics Letters A*, vol. 319, no. 3-4, pp. 373–378, 2003.

[19] A. Kanel-Belov, A. Dyskin, Y. Estrin, E. Pasternak, and I. A. Ivanov-Pogodaev, "Interlocking of convex polyhedra: towards a geometric theory of fragmented solids," *arXiv preprint arXiv:0812.5089*, 2008.

[20] A. Dyskin, E. Pasternak, and Y. Estrin, "Topological interlocking as a design principle for hybrid materials," in *Proceedings of the 8th Pacific Rim International Congress on Advanced Materials and Processing*, pp. 1525–1534, Springer, 2013.

[21] A. Dyskin, Y. Estrin, A. Kanel-Belov, and E. Pasternak, "A new principle in design of composite materials: reinforcement by interlocked elements," *Composites Science and Technology*, vol. 63, no. 3-4, pp. 483–491, 2003.

[22] A. V. Dyskin, Y. Estrin, E. Pasternak, H. C. Khor, and A. J. Kanel-Belov, "Fracture resistant structures based on topological interlocking with non-planar contacts," *Advanced Engineering Materials*, vol. 5, no. 3, pp. 116–119, 2003.

[23] Y. Estrin, A. V. Dyskin, E. Pasternak, H. C. Khor, and A. J. Kanel-Belov, "Topological interlocking of protective tiles for the space shuttle," *Philosophical magazine letters*, vol. 83, no. 6, pp. 351–355, 2003.

[24] V. Piirainen and Y. Estrin, "New approach to road construction in oil-producing regions of western siberia," in *IOP Conference Series: Earth and Environmental Science*, vol. 87/7, p. 072003, IOP Publishing, 2017.

[25] A. Dyskin, Y. Estrin, and E. Pasternak, *Topological Interlocking Materials*, pp. 23–49. Springer Series in Materials Science, 01 2019.

[26] A. V. Dyskin, E. Pasternak, and Y. Estrin, "Mortarless structures based on topological interlocking," *Frontiers of Structural and Civil Engineering*, vol. 6, no. 2, pp. 188–197, 2012.

[27] A. V. Dyskin, H. C. Khor, D. Yong, E. Pasternak, Y. Estrin, and A. Kanel-Belov, "Deployable interlocking structures for martian bases," *Proceedings of 7th Australian Mars Exploration Conference*, 2007.

[28] B. Zareiyan and B. Khoshnevis, "Effects of interlocking on interlayer adhesion and strength of structures in 3d printing of concrete," *Automation in Construction*, vol. 83, pp. 212–221, 2017.

[29] A. V. Dyskin, Y. Estrin, A. J. Kanel-Belov, and E. Pasternak, "Toughening by fragmentation—how topology helps," *Advanced Engineering Materials*, vol. 3, no. 11, pp. 885–888, 2001.

[30] Y. Estrin, A. Dyskin, E. Pasternak, and S. Schaare, "Topological interlocking in design of structures and materials," *MRS Online Proceedings Library Archive*, vol. 1188, 2009.

[31] Y. Estrin, A. Dyskin, A. Kanel-Belov, and E. Pasternak, "Materials with novel architectonics: Assemblies of interlocked elements," in *IUTAM Symposium on Analytical and Computational Fracture Mechanics of Non-homogeneous Materials*, pp. 51–55, Springer, 2002.

[32] H. Khor, A. Dyskin, Y. Estrin, and E. Pasternak, "Mechanisms of fracturing in structures built from topologically interlocked blocks," *SIF2004 Structural Integrity and Fracture*, 2004.

[33] A. Dyskin and A. Caballero, "Orthogonal crack approaching an interface," *Engineering fracture mechanics*, vol. 76, no. 16, pp. 2476–2485, 2009.

[34] J.-G. Gallon, *Machines et inventions approuvées par l'Academie Royale des Sciences depuis son établissement jusqu'à présent; avec leur description*, vol. 7. chez Gabriel Martin, Jean-Baptiste Coignard, fils, Hippolyte-Louis Guerin . . . , 1777.

[35] A. Borhani and N. Kalantar, "'apart but together: The interplay of geometric relationships in aggregated interlocking systems'," in *ShoCK!-Sharing Computational Knowledge!: Proceedings of the 35th eCAADe Conference*, vol. 1, pp. 639–648, 2017.

[36] I. M. Vella and T. Kotnik, "Stereotomy, an early example of a material system," *Sharing of Computable Knowledge!*, pp. 251–259, 2017.

[37] A. V. Dyskin, Y. Estrin, A. J. Kanel-Belov, and E. Pasternak, "Topological interlocking of platonic solids: A way to new materials and structures," *Philosophical magazine letters*, vol. 83, no. 3, pp. 197–203, 2003.

[38] A. Dyskin, Y. Estrin, and E. Pasternak, "Topological interlocking materials," in *Architectured Materials in Nature and Engineering*, pp. 23–49, Springer, 2019.

[39] D. Yeomans, "The serlio floor and its derivations," *arq: Architectural Research Quarterly*, vol. 2, no. 3, pp. 74–83, 1997.

[40] A. Pugnale, D. Parigi, P. H. Kirkegaard, and M. S. Sassone, "The principle of structural reciprocity: history, properties and design issues," in *The 35th Annual Symposium of the IABSE 2011, the 52nd Annual Symposium of the IASS 2011 and incorporating the 6th International Conference on Space Structures*, pp. 414–421, 2011.

[41] M. Brocato and L. Mondardini, "A new type of stone dome based on abeille's bond," *International Journal of Solids and Structures*, vol. 49, no. 13, pp. 1786–1801, 2012.

[42] M. Weizmann, O. Amir, and Y. J. Grobman, "Topological interlocking in buildings: A case for the design and construction of floors," *Automation in Construction*, vol. 72, pp. 18–25, 2016.

[43] R. Evans, *The projective cast: architecture and its three geometries*. MIT press, 1995.

[44] O. Baverel, H. Nooshin, Y. Kuroiwa, and G. Parke, "Nexorades," *International Journal of Space Structures*, vol. 15, no. 2, pp. 155–159, 2000.

[45] M. Brocato and L. Mondardini, "Parametric analysis of structures from flat vaults to reciprocal grids," *International Journal of Solids and Structures*, vol. 54, pp. 50–65, 2015.

[46] A. Frézier, "1737 (ed. 1980): La théorie et la pratique de la coupe des pierres et des bois pour la construction des voûtes et autres parties des bâtiments civils et militaires," *Nogent-le-Roy: Jacques Laget LAME*, 1737.

[47] I. Miadragovič Vella, T. Kotnik, A. Herneoja, T. Österlund, P. Markkanen, *et al.*, "Geometric versatility of abeille vault," *eCAADe 2016*, 2016.

[48] M. Brocato, W. Deleporte, L. Mondardini, and J.-E. Tanguy, "A proposal for a new type of prefabricated stone wall," *International Journal of Space Structures*, vol. 29, no. 2, pp. 97–112, 2014.

[49] M. Brocato and L. Mondardini, "Geometric methods and computational mechanics for the design of stone domes based on abeille's bond," *Advances in Architectural Geometry 2010*, pp. 149–162, 2010.

[50] E. R. Dìaz, "La bóveda plana de abeille en lugo," in *Actas del Segundo Congreso Nacional de Historia de la Construcción, A Coruna*, pp. 22–24, 1998.

[51] G. Fallacara, "Digital stereotomy and topological transformations: reasoning about shape building," in *Proceedings of the second international congress on construction history*, vol. 1, pp. 1075–1092, 2006.

[52] M. Senechal, "Which tetrahedra fill space?," *Mathematics Magazine*, vol. 54, no. 5, pp. 227–243, 1981.

[53] M. Gardner, *Sixth book of mathematical games from Scientific American*. WH Freeman San Francisco, 1971.

[54] M. Goldberg, "The space-filling pentahedra," *Journal of Combinatorial Theory, Series A*, vol. 13, no. 3, pp. 437–443, 1972.

[55] M. Goldberg, "Convex polyhedral space-fillers of more than twelve faces," *Geometriae Dedicata*, vol. 8, no. 4, pp. 491–500, 1979.

[56] M. Goldberg, "On the space-filling enneahedra," *Geometriae Dedicata*, vol. 12, no. 3, pp. 297–306, 1982.

[57] R. E. Williams, "Space-filling polyhedron: its relation to aggregates of soap bubbles, plant cells, and metal crystallites," *Science*, vol. 161, no. 3838, pp. 276–277, 1968.

[58] R. Williams, *The geometrical foundation of natural structure: A source book of design*. Dover New York, 1979.

[59] N. W. Johnson, "Convex polyhedra with regular faces," *Canadian Journal of Mathematics*, vol. 18, pp. 169–200, 1966.

[60] S. Alvarez, "The gyrobifastigium, not an uncommon shape in chemistry," *Coordination Chemistry Reviews*, vol. 350, pp. 3–13, 2017.

[61] H. S. M. Coxeter, *Regular polytopes*. Courier Corporation, 1973.

[62] T. W. Sederberg and E. Greenwood, "A physically based approach to 2–d shape blending," *ACM SIGGRAPH computer graphics*, vol. 26, no. 2, pp. 25–34, 1992.

[63] T. W. Sederberg, P. Gao, G. Wang, and H. Mu, "2-d shape blending: an intrinsic solution to the vertex path problem," *Proceedings of the 20th annual conference on Computer graphics and interactive techniques*, pp. 15–18, 1993.

[64] M. Alexa, D. Cohen-Or, and D. Levin, "As-rigid-as-possible shape interpolation," in *Proceedings of the 27th annual conference on Computer graphics and interactive techniques*, pp. 157–164, ACM Press/Addison-Wesley Publishing Co., 2000.

[65] G. Turk and J. F. O'brien, "Shape transformation using variational implicit functions," in *ACM SIGGRAPH 2005 Courses*, p. 13, ACM, 2005.

[66] C. Schumacher, S. Marschner, M. Cross, and B. Thomaszewski, "Mechanical characterization of structured sheet materials," *ACM Trans. Graph.*, vol. 37, pp. 148:1–148:15, July 2018.

[67] C. S. Kaplan, "Voronoi diagrams and ornamental design," in *in The First Annual Symposium of the International Society for the Arts, Mathematics, and Architecture*, pp. 277–283, 2000.

[68] M. Rao, "Exhaustive search of convex pentagons which tile the plane." arXiv preprint arXiv:1708.00274, 2017.

[69] H. L. et al., "Spatial modeling of bone microarchitecture," *Proceedings Volume 8290, Three-Dimensional Image Processing (3DIP) and Applications II*, vol. 8290, 2012.

[70] S. AlZu'bi and A. Amira, "3d medical volume segmentation using hybrid multiresolution statistical approaches," *Adv. Artificial Intellegence*, vol. 2010, 07 2010.

[71] D.-M. Yan, W. Wang, B. Lévy, and Y. Liu, "Efficient computation of 3d clipped voronoi diagram," in *International Conference on Geometric Modeling and Processing*, pp. 269–282, Springer, 2010.

[72] G. Rong and T.-S. Tan, "Jump flooding in gpu with applications to voronoi diagram and distance transform," in *Proceedings of the 2006 Symposium on Interactive 3D Graphics and Games*, I3D '06, (New York, NY, USA), p. 109–116, Association for Computing Machinery, 2006.

[73] F. Aurenhammer, G. Paulini, and B. Jüttler, "Voronoi diagrams for parallel halflines in 3d," in *Proceedings of the 32nd European Workshop on Computational Geometry EuroCG'2016*, 3 2016.

[74] H. Everett, D. Lazard, S. Lazard, and M. Safey El Din, "The voronoi diagram of three lines," *Discrete & Computational Geometry*, vol. 42, 06 2007.

[75] D. Dutta and C. M. Hoffmann, "A geometric investigation of the skeleton of csg objects," tech. rep., MICHIGAN UNIV ANN ARBOR, 1990.

[76] G. Elber, E. Cohen, and S. Drake, "Mathsm: medial axis transform toward high speed machining of pockets," *Computer-Aided Design*, vol. 37, no. 2, pp. 241 – 250, 2005.

[77] V. Koltun and M. Sharir, "Three dimensional euclidean voronoi diagrams of lines with a fixed number of orientations," in *Proceedings of the Eighteenth Annual Symposium on Computational Geometry*, SCG '02, (New York, NY, USA), pp. 217–226, ACM, 2002.

[78] C. Icking and L. Ma, "A tight bound for the complexity of voronoi diagrams under polyhedral convex distance functions in 3d," *Conference Proceedings of the Annual ACM Symposium on Theory of Computing*, pp. 316–321, 01 2001.

[79] J.-P. Luminet and B. F. Roukema, "Topology of the universe: Theory and observation," in *Theoretical and Observational Cosmology*, pp. 117–156, Springer, 1999.

[80] E. Cohen, R. F. Riesenfeld, and G. Elber, *Geometric modeling with splines: an introduction*. AK Peters/CRC Press, 2001.

[81] F. Massarwi and G. Elber, "A b-spline based framework for volumetric object modeling," *Computer-Aided Design*, vol. 78, no. C, pp. 36–47, 2016.

[82] E. Akleman and J. Chen, "Generalized distance functions," in *Proceedings Shape Modeling International'99. International Conference on Shape Modeling and Applications*, pp. 72–79, IEEE, 1999.

[83] H. Nyquist, "Certain topics in telegraph transmission theory," *Transactions of the American Institute of Electrical Engineers*, vol. 47, no. 2, pp. 617–644, 1928.

[84] B. N. Boots, "Delaunay triangles: an alternative approach to point pattern analysis," *Proceedings of the Association of American Geographers*, vol. 6, pp. 26–29, 1974.

[85] D. F. Watson, "Computing the n-dimensional delaunay tessellation with application to voronoi polytopes," *The computer journal*, vol. 24, no. 2, pp. 167–172, 1981.

[86] L. Guibas and J. Stolfi, "Primitives for the manipulation of general subdivisions and the computation of voronoi," *ACM transactions on graphics (TOG)*, vol. 4, no. 2, pp. 74–123, 1985.

[87] B. Grünbaum and G. C. Shephard, *Tilings and patterns*. Freeman, 1987.

[88] S. Khandelwal, T. Siegmund, R. Cipra, and J. Bolton, "Transverse loading of cellular topologically interlocked materials," *International Journal of Solids and Structures*, vol. 49, no. 18, pp. 2394–2403, 2012.

[89] R. v. Mises, "Mechanics of solid bodies in the plastically-deformable state," *Göttin Nachr Math Phys*, vol. 1, pp. 582–592, 1913.

[90] E. Akleman, J. Chen, Q. Xing, and J. Gross, "Cyclic plain-weaving with extended graph rotation systems," *ACM Transactions on Graphics; Proceedings of SIGGRAPH'2009*, pp. 78.1–78.8, August 2009.

[91] M. Ebert, S. G. Subramanian, E. Akleman, and V. R. Krishnamurthy, "Generative infills for additive manufacturing using space-filling polygonal tiles," *International Design Engineering Technical Conferences & Computers and Information in Engineering*, 2020.

[92] E. Akleman, J. Chen, Q. Xing, and J. Gross, "Cyclic plain-weaving with extended graph rotation systems," *ACM Transactions on Graphics; Proceedings of SIGGRAPH'2009*, vol. 28, pp. 78.1–78.8, August 2009.

[93] E. Akleman, J. Chen, and J. L. Gross, "Extended graph rotation systems as a model for cyclic weaving on orientable surfaces," *Discrete Applied Mathematics*, vol. 193, pp. 61–79, 2015.

[94] R. Roelofs, "Three-dimensional and dynamic constructions based on leonardo grids," *International Journal of Space Structures*, vol. 22, no. 3, pp. 191–200, 2007.

[95] M. Conder and P. Dobcsányi, "Determination of all regular maps of small genus," *Journal of Combinatorial Theory, Series B*, vol. 81, no. 2, pp. 224–242, 2001.

[96] J. J. Van Wijk, "Symmetric tiling of closed surfaces: Visualization of regular maps," *ACM Transactions on Graphics (TOG)*, vol. 28, no. 3, p. 49, 2009.

[97] V. R. Krishnamurthy, E. Akleman, S. G. Subramanian, K. Boyd, C.-a. Fu, M. Ebert, C. Startett, and N. Yadav, "Bi-axial woven tiles: Interlocking space-filling shapes based on symmetries of bi-axial weaving patterns," in *Proceedings of the 46th graphics interface conference, GI*, 2020.

[98] J. I. Lipton, R. MacCurdy, Z. Manchester, L. Chin, D. Cellucci, and D. Rus, "Handedness in shearing auxetics creates rigid and compliant structures," *Science*, vol. 360, no. 6389, pp. 632–635, 2018.

[99] C. S. Ha, M. E. Plesha, and R. S. Lakes, "Chiral three-dimensional isotropic lattices with negative poisson's ratio," *physica status solidi (b)*, vol. 253, no. 7, pp. 1243–1251, 2016.

[100] W. Wu, W. Hu, G. Qian, H. Liao, X. Xu, and F. Berto, "Mechanical design and multifunctional applications of chiral mechanical metamaterials: A review," *Materials & Design*, vol. 180, p. 107950, 2019.

[101] E. Renuart and C. Viney, "Biological fibrous materials: Self-assembled structures and optimised properties," in *Structural Biological Materials (Edited by M. Elices)*, pp. 221–267, Oxford, UK: Pergamon/Elsevier Science, 2000.

[102] Y. Liu, M. O'Keeffe, M. M. Treacy, and O. M. Yaghi, "The geometry of periodic knots, polycatenanes and weaving from a chemical perspective: a library for reticular chemistry," *Chemical Society Reviews*, vol. 47, no. 12, pp. 4642–4664, 2018.

[103] P. Gailiunas, "Mad weave," *Journal of Mathematics and the Arts*, vol. 11, no. 1, pp. 40–58, 2017.

[104] A. Airoldi, P. Bettini, P. Panichelli, M. F. Oktem, and G. Sala, "Chiral topologies for composite morphing structures–part i: Development of a chiral rib for deformable airfoils," *physica status solidi (b)*, vol. 252, no. 7, pp. 1435–1445, 2015.

[105] A. Airoldi, P. Bettini, P. Panichelli, and G. Sala, "Chiral topologies for composite morphing structures–part ii: Novel configurations and technological processes," *physica status solidi (b)*, vol. 252, no. 7, pp. 1446–1454, 2015.

[106] S. Wheeland, F. Bayatpur, A. V. Amirkhizi, and S. Nemat-Nasser, "Chiral braided and woven composites: design, fabrication, and electromagnetic characterization," in *Behavior and Mechanics of Multifunctional Materials and Composites 2011* (Z. Ounaies and S. S. Seelecke, eds.), vol. 7978, pp. 278 – 282, International Society for Optics and Photonics, SPIE, 2011.

[107] A. Pugnale and M. Sassone, "Structural reciprocity: critical overview and promising research/design issues," *Nexus Network Journal*, vol. 16, no. 1, pp. 9–35, 2014.

[108] P. Song, C.-W. Fu, P. Goswami, J. Zheng, N. J. Mitra, and D. Cohen-Or, "Reciprocal frame structures made easy," *ACM Transactions on Graphics (TOG)*, vol. 32, no. 4, pp. 1–13, 2013.

[109] D. J. Kasik, W. Buxton, and D. R. Ferguson, "Ten cad challenges," *IEEE Computer Graphics and Applications*, vol. 25, no. 2, pp. 81–92, 2005.